Supplementary figure 1

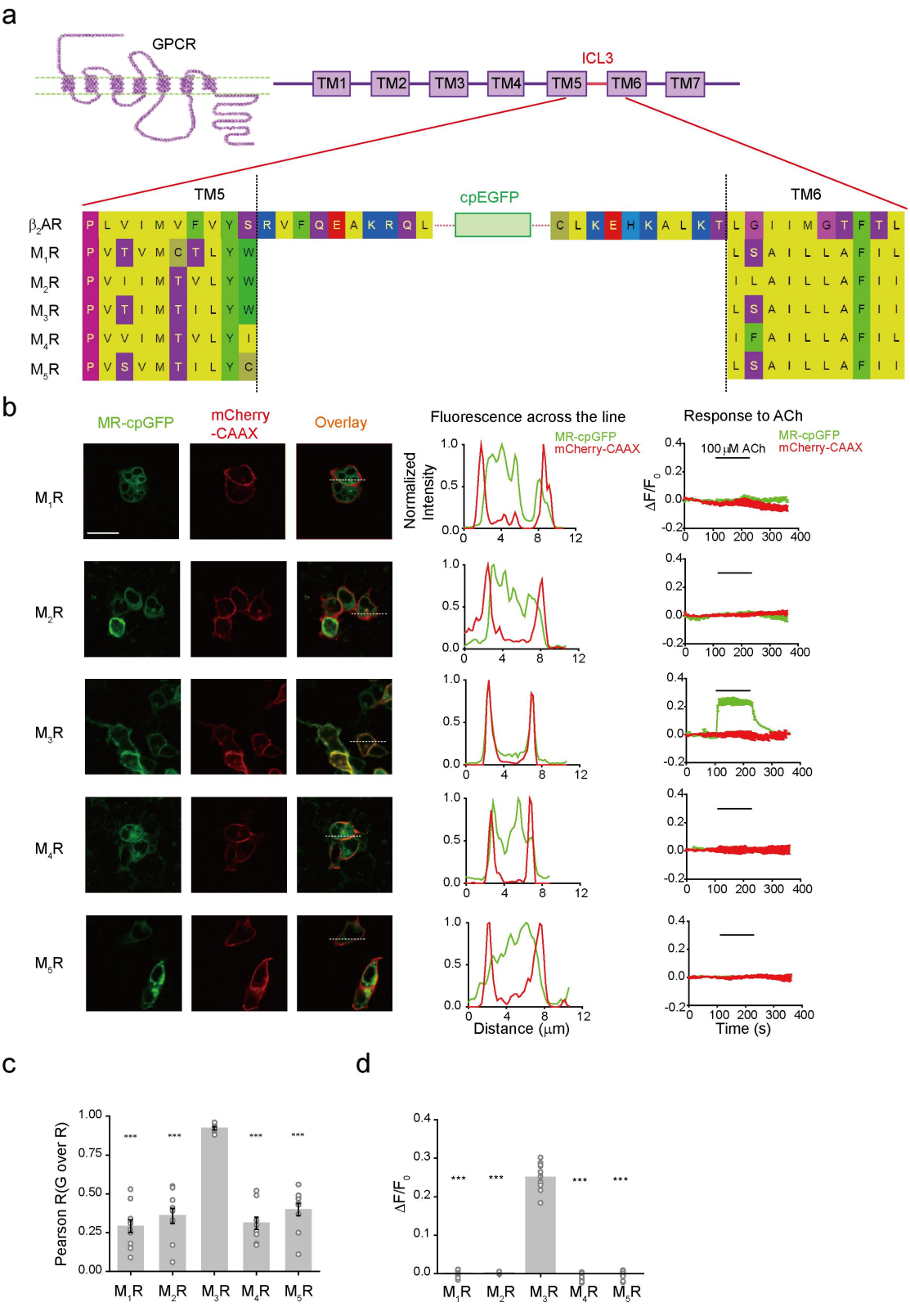

Supplementary figure 1: Screening the prototypes for GACh sensors, related to Fig. 1.

(**a**) Sequencing alignments of regions between TM5 and TM6 of β_2AR and $M_{1\text{-}5}$Rs. β_2 ICL_3 was grafted into $M_{1\text{-}5}$Rs as indicated by black dash lines. The ICL_3 were defined according to the UNIPROT database.

(**b**) Left, representative snapshots of HEK293T cells co-transfected with $M_{1\text{-}5}$R-based chimeric sensors and mCherry-CAAX in green and red channels. Middle plots show GFP and mCherry fluorescence in transfected HEK293T cells along the scan lines indicated in left snapshots. Right, fluorescence responses in transfected HEK293T cells after bath application of 100 μM ACh.

(**c**) Quantification of the colocalization of $M_{1\text{-}5}$R based sensors and mCherry-CAAX. Pearson colocalization ratio M_1R (0.29 ± 0.04, *n* = 10 cells from 2 cultures, *U* = 110, *p* = 1.22E-4), M_2R (0.36 ± 0.05, *n* = 9 cells from 2 cultures, *U* = 99, *p* = 1.94E-4), M_4R (0.31 ± 0.04, *n* = 8 cells from 2 cultures, *U* = 88, *p* = 3.22E-4), and M_5R (0.40 ± 0.04, *n* = 10 cells from 2 cultures, *U* = 110, *p* = 1.22E-6) compared with M_3R (0.92 ± 0.01, *n* = 11 cells from 2 cultures).

(**d**) Quantification of ACh-evoked $\Delta F/F_0$ responses in $M_{1\text{-}5}$R expressing cells in (**b**). $\Delta F/F_0$ of M_1R (0.03 ± 0.22%, *n* = 14 cells from 2 cultures, *U* = 168, *p* = 1.75E-5), M_2R (0.17 ± 0.04%, *n* = 13 cells from 2 cultures, *U* = 156, *p* = 2.49E-5), M_4R (-1.1 ± 0.24%, *n* = 14 cells from 2 cultures, *U* = 168, *p* = 1.75E-5), and M_5R (-0.13 ± 0.24%, *n* = 15 cells from 2 cultures, *U* = 180, *p* = 1.26E-5) compared with that of M_3R (25.1 ± 0.88%, *n* = 12 cells from 2 cultures).

Data are shown with mean ± s.e.m, with error bars indicate s.e.m.

*, $p < 0.05$, **, $p < 0.01$, ***, $p < 0.001$, n.s., not significant (Mann-Whitney Rank Sum non-parametric tests, two-sides). Scale bar: 10 μm.

Supplementary figure 2:

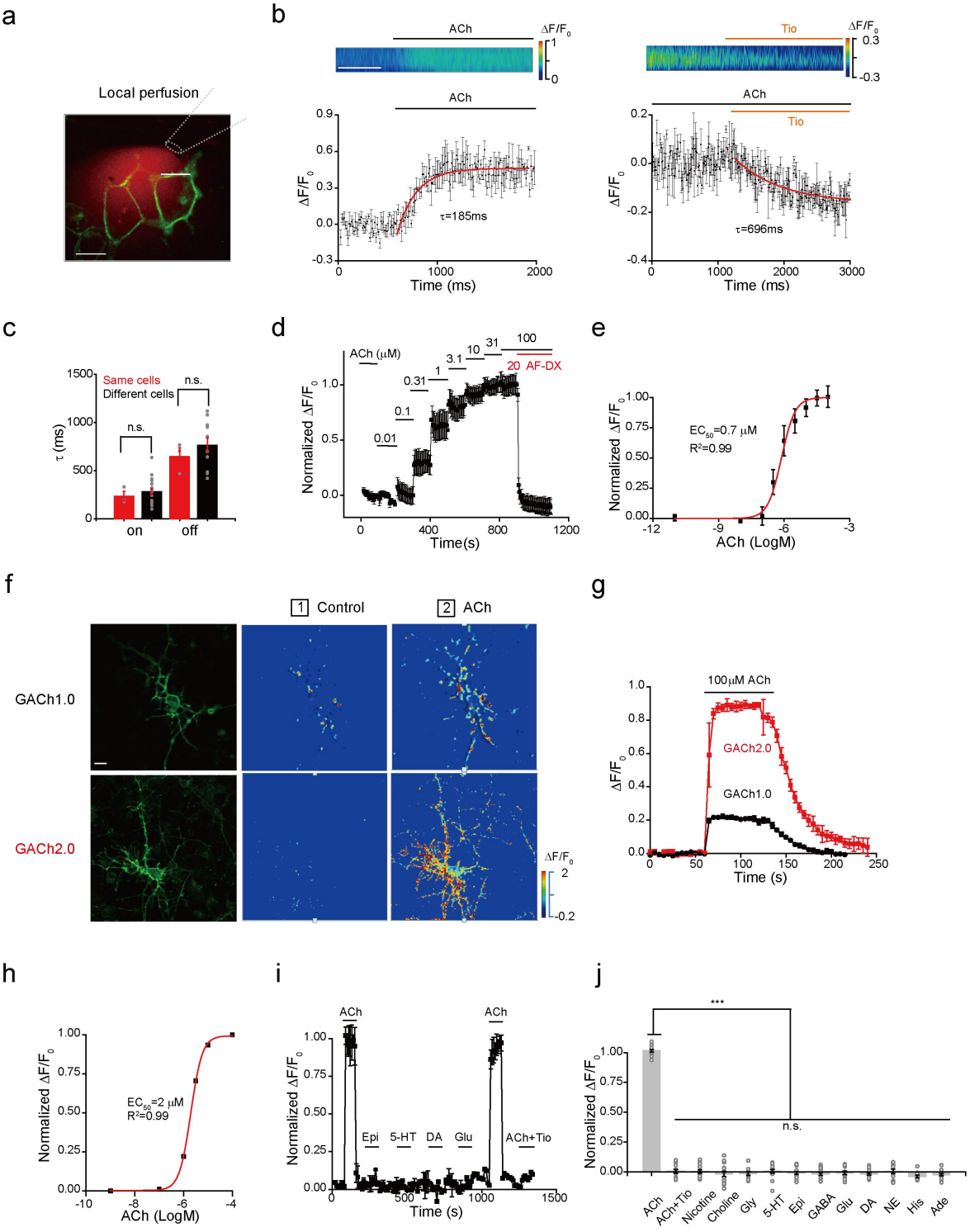

Supplementary figure 2：Optimization of GACh1.0 through linker randomization, related to Fig. 1.

(**a**) Left, the two- and five-amino acid linkers that connect the N and C termini of cpGFP were individually randomized to 20 possible amino acids. Right, randomized mutations generated 1-4 top hits from each residue (red).

(**b**) The respective sequence information and $\Delta F/F_0$ responses from the 23 candidates in the second-round screening (*n* = 4 cells from 2 cultures), during which GACh2.0 (red) exhibited $\Delta F/F_0$ of ~0.9.

Data are shown with mean ± s.e.m, with error bars indicate s.e.m.

Supplementary figure 3

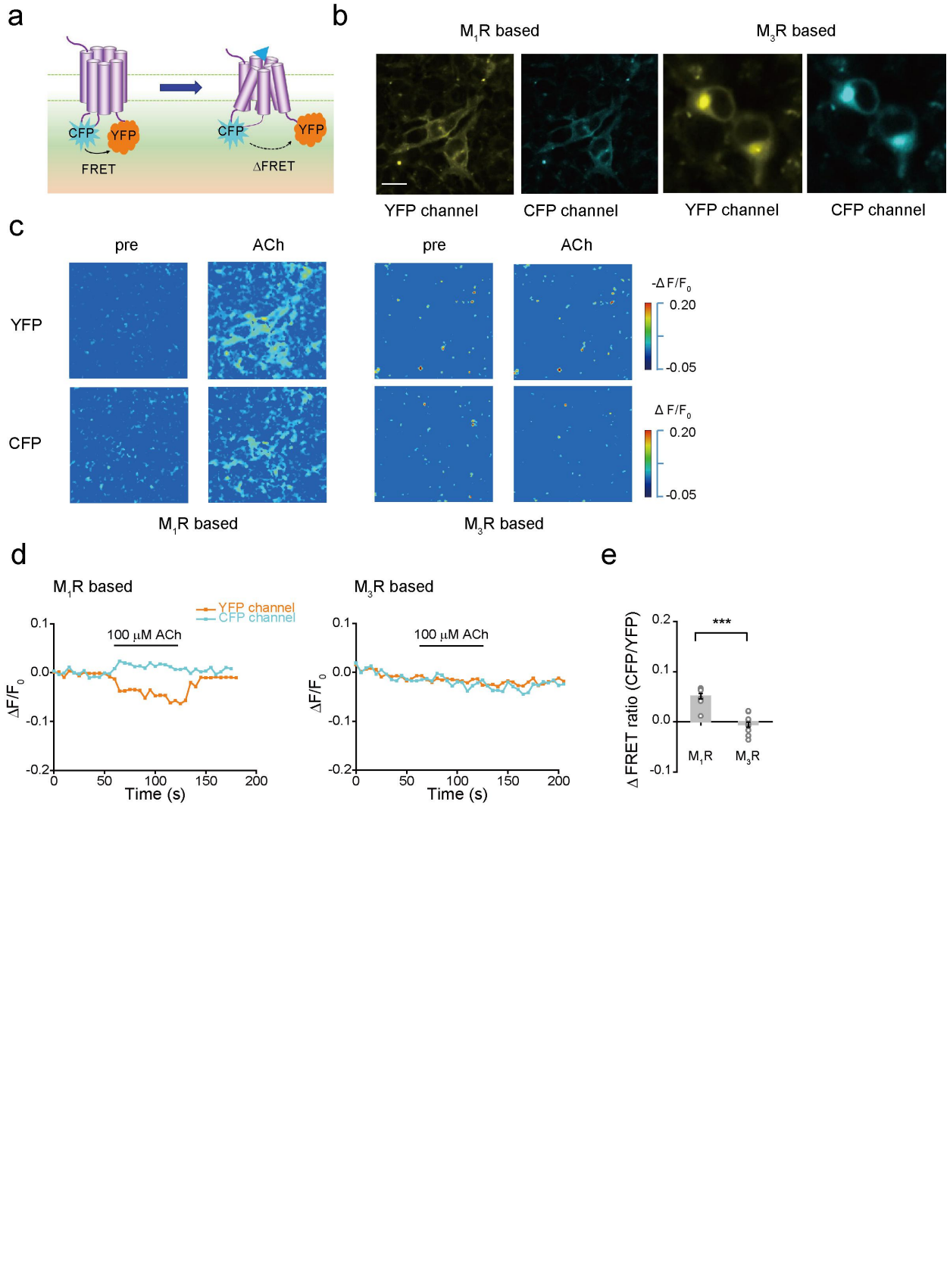

Supplementary figure 3: MR-based FRET sensors respond poorly to ACh, related to Fig. 1.

(**a**) Schematic illustration of the principle of MR-based FRET sensors.

(**b**) Snapshots of M_1R- and M_3R-based FRET sensors expressed in HEK293T cells in YFP and CFP channels. Note the significant intracellular retention of M_3R-based FRET sensors (right).

(**c**) Pseudocolor snapshots of M_1R- and M_3R-based FRET sensors with or without ACh treatment. Note the YFP channel processed with $-\Delta F/F_0$ in pseudocolor.

(**d**) Fluorescence responses of HEK293T cells expressing M_1R-based (n = 10 cells from 8 cultures) and M_3R-based (n = 14 cells from 4 cultures) FRET sensors to application of 100 μM ACh in YFP and CFP channels.

(**e**) Quantification of the changes in FRET ratio (CFP/YFP) to ACh application (M_1R-based sensor: 5.1 ± 0.55%, n = 10 cells from 8 cultures; M_3R-based sensor: -0.53 ± 0.49%, n = 14 cells from 4 cultures, U = 137, p = 9.87E-5).

Data are shown with mean ± s.e.m, with error bars indicate s.e.m. Experiments in (**b**),(**c**) were repeated independently for more than 4 cultures with similar results.

***, $p < 0.001$ (Mann-Whitney Rank Sum non-parametric tests, two-sides).

Supplementary figure 4

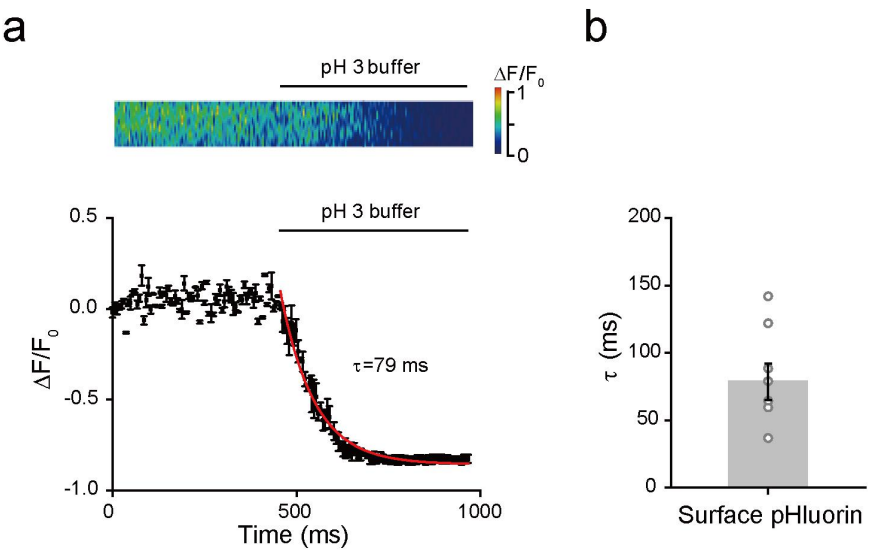

Supplementary figure 4: System delay of the local perfusion system, related to Fig. 2.

(**a**) Upper, fluorescence responses of a pH-sensitive fluorescent protein pHluorin expressing HEK293T cell to local perfusion of a pH 3 acidic buffer. Lower plot shows the decay of fluorescence responses of the expressing cell (averaged from 3 ROIs in the same cell).

(**b**) Decay time constants of pHluorin expressing cells to local perfusion of acidic buffer (78.7 ± 13.4 ms; *n* = 8 cells from 8 cultures).

Data are shown with mean ± s.e.m, with error bars indicate s.e.m.

Supplementary figure 5

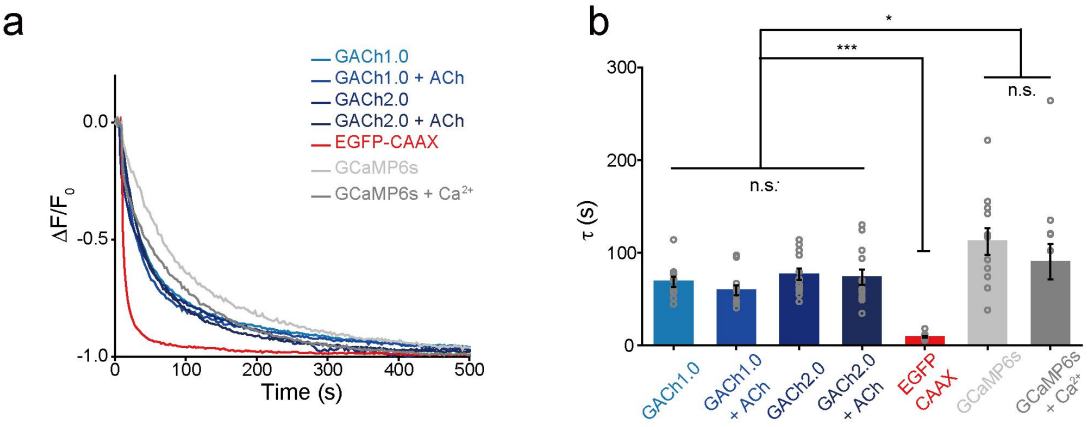

Supplementary figure 5: GACh sensors have comparable photostability with other GFP-based probes

(a) Representative photo-bleaching curves of GACh1.0, GACh2.0, EGFP-CAAX and GCaMP6s expressed in HEK293T cells under confocal microscope. GACh1.0 and GACh2.0 were tested with or without 100 μM ACh application. GCaMP6s was tested with or without 2 mM external Ca^{2+}, and digitonin (10 μg/ml) was used to permeabilize the plasma membrane. Whole cells were selected as the ROI for bleaching and the 488 nm laser was used with ~350 uW power.

(b) Quantification of decay time constants for different probes (GACh1.0: 68.7 ± 5.59 s, *n* = 11 cells from 11 cultures, GACh1.0+ACh: 59.6 ± 5.03 s, *n* = 13 cells from 13 cultures, GACh2.0: 76.7 ± 6.10 s, *n* = 13 cells from 13 cultures, GACh2.0+ACh: 73.4 ± 8.32 s, *n* = 13 cells from 13 cultures. EGFP-CAAX: 9.07 ± 0.92 s, *n* = 13 cells from 13 cultures, *U* = 169, *p* = 1.69E-5 compared with GACh2.0. GCaMP6s: 112.3 ± 14.3 s, *n* = 12 cells from 12 cultures. GCaMP6s+2 mM Ca^{2+}: 90.3 ± 19.2 s, *n* = 12 cells from 12 cultures, *U* = 39, *p* = 0.036 compared with GACh2.0).

Data are shown with mean ± s.e.m, with error bars indicate s.e.m. Experiments in (**b**) were repeated independently for more than 10 cultures with similar results.

*, $p < 0.05$, **, $p < 0.01$, ***, $p < 0.001$, n.s., not significant (Mann-Whitney Rank Sum non-parametric tests, two-sides).

Supplementary figure 6

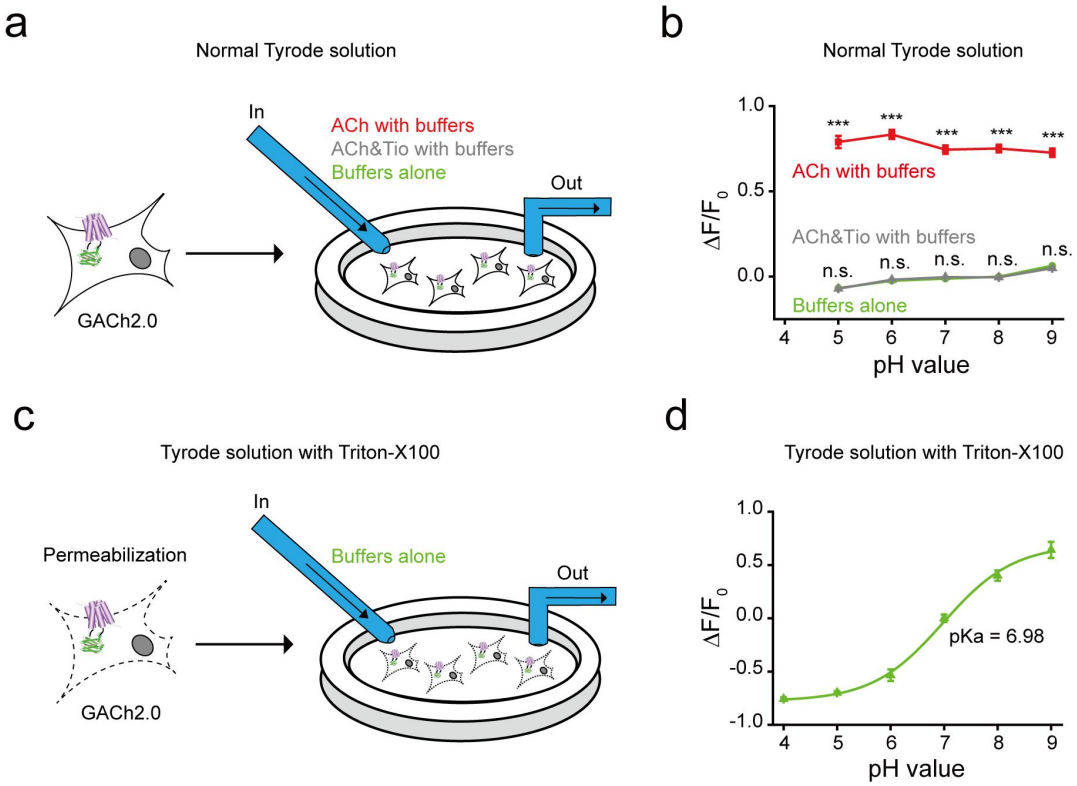

Supplementary figure 6: The effect of pH on GACh2.0 signals.

(**a**) Schematic illustration of the experimental design used to measure the effects of bath applied ACh (red), ACh&Tio (gray), and/or buffers alone (green) on fluorescence responses in GACh2.0 expressing HEK293T cells.

(**b**) Quantification for ACh-, ACh&Tio- and/or buffer-induced fluorescence responses collected from 2 cultures of 9 cells (pH 5 buffer: -6.81 ± 0.78%; +ACh: 78.90 ± 3.60%; +ACh&Tio: -7.12 ± 0.66%; pH 6 buffer: -2.52 ± 0.78%; +ACh:83.32 ± 2.67%; +ACh&Tio: -1.88 ± 0.19%; pH 7 buffer: -1.26 ± 0.17%; +ACh: 74.44 ± 2.43%; +ACh&Tio: -0.39 ± 0.12%; pH 8 buffer: 0.08 ± 0.08%; +ACh: 75.09 ± 2.27%; +ACh&Tio: -0.45 ± 0.72%; pH 9 buffer: 6.33 ± 0.83%; +ACh: 72.65 ± 2.45%;

+ACh&Tio: 4.91 ± 0.65%). Note the much larger ACh-induced fluorescence responses compared to the buffer-induced ones under all pH conditions (*U* = 143 for pH 5, *p* = 3.90E-5; *U* = 165 for pH 6, *p* = 2.08E-5 ; *U* = 216 for pH 7, *p* = 5.34E-6; *U* = 208 for pH 8, *p* = 5.66E-6; *U* = 154 for pH 9; *p* = 2.81E-5).

(**c**) Schematic illustration of the experimental design used to measure the effects of bath applied buffers (green) on fluorescence responses in GACh2.0 expressing HEK293T cells gently permeabilized by detergent Triton-X100 (0.3% for 5 minutes).

(**d**) Quantification for the relative buffer-induced fluorescence responses collected from 6 plate wells of ~200 cells. The fluorescence intensity of pH 7 was set as F_0 and the relative fluorescence changes in each pH value were plotted (pH 4: -0.76 ± 0.02, pH 5: -0.70 ± 0.02, pH 6: -0.53 ± 0.05, pH 7: 0.00 ± 0.04, pH 8: 0.40 ± 0.05, pH 9: 0.64 ± 0.08).

Data are shown with mean ± s.e.m, with error bars indicate s.e.m.

***, $p < 0.001$, n.s., not significant (Mann-Whitney Rank Sum non-parametric tests, two-sides).

Supplementary figure 7

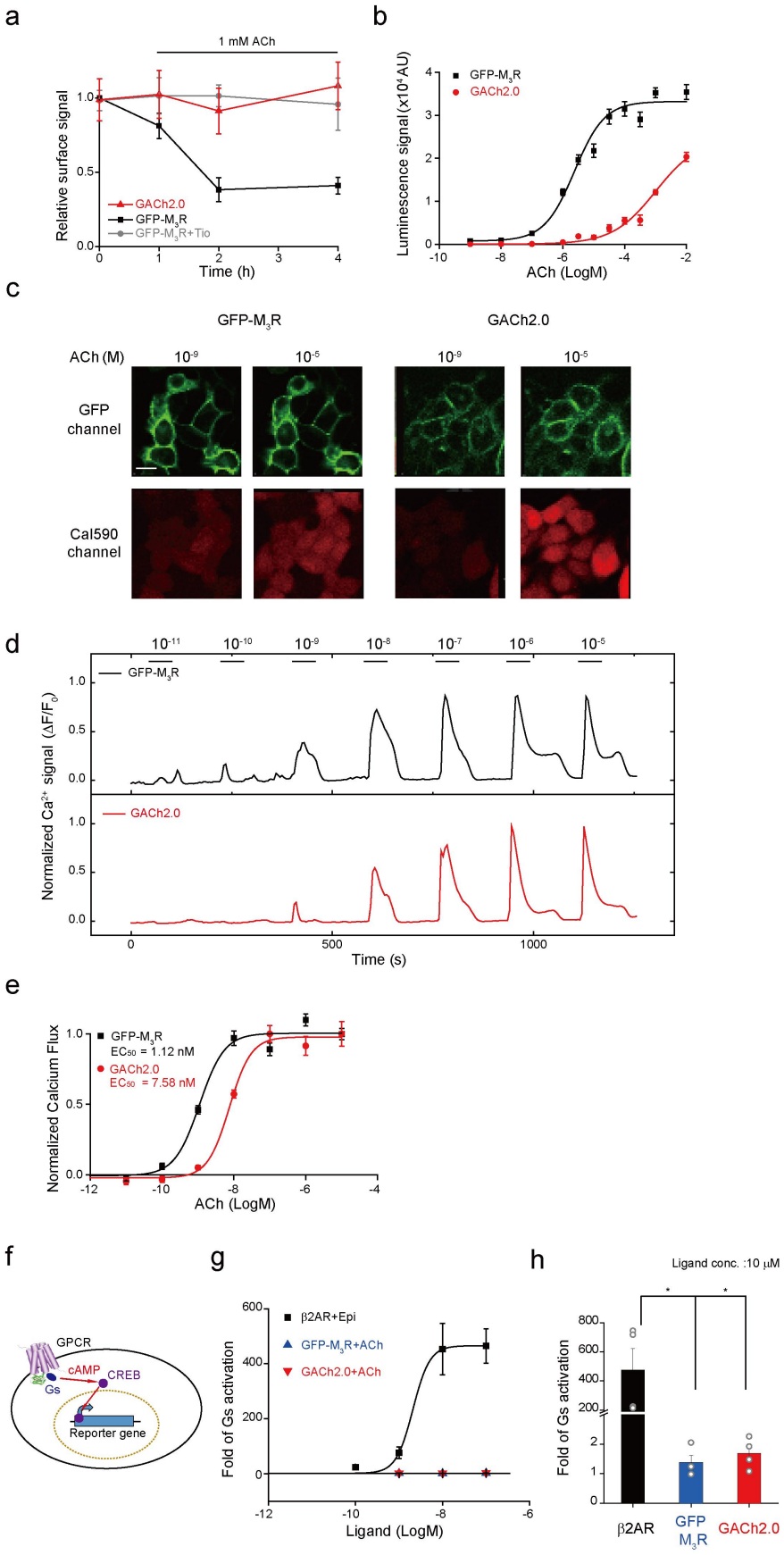

Supplementary figure 7: GACh has negligible M_3R activation-dependent internalization and decreased coupling to G protein in HEK293T cells.

(**a**) Plots of fluorescence intensity of GACh2.0 or GFP tagged wild type M_3R (GFP-M_3R) expressing cells in the normal bath solution or solution containing 20 μM tiotropium (Tio) against the time of application of 1 mM ACh (*n* = 48 wells/time point, >100 cells/well).

(**b**) The reporter luminescence response-ACh concentration relationships and EC_{50} (GFP-M_3R: 2.3 ± 0.49 μM; GACh2.0: 537 ± 94 μM; *n* = 4 wells/concentration, *U* = 16, *p* = 0.029) of GFP-M_3R and GACh2.0 expressing cells.

(**c**) Images show membrane expression (GFP channel) and Ca^{2+} responses (red Cal-590 channel) of GFP-M_3R and GACh2.0 expressing HEK293T cells to application of 0.1 and 100 μM ACh.

(**d**) Ca^{2+} responses of GFP-M_3R and GACh2.0 expressing HEK293T cells to increasing concentrations of ACh.

(**e**) The ACh concentration-Ca^{2+} responses relationships and calculated EC_{50} of GFP-M_3R and GACh2.0 expressing HEK293T cells (EC_{50}: GFP-M_3R: 1.12 ± 0.08 nM; GACh2.0: 7.58 ± 0.41 nM; *n* = 22 cells; *U* = 484, *p* = 1.27E-8).

(**f**) Schematic illustration of NanoLuc-based reporter gene assay used to detect GPCR-coupled Gs pathway.

(**g**) Reporter signal seen in β_2AR expressing cells to bath application of epinephrine, but not in GACh2.0 and GFP-M_3R expressing cells to bath application of ACh (*n* = 4 wells with >100 cells each well).

(**h**) Quantification of fold increases of luciferase signals with 10 μM ligand (β_2AR: 464.9 ± 62.5, GFP-M_3R: 2.96 ± 0.53, GACh2.0: 2.23 ± 0.24, n = 4 wells for each group, U = 16, p = 0.03).

Data are shown with mean ± s.e.m, with error bars indicate s.e.m. All scale bars: 10 μm

Experiments in (**c**),(**d**) were repeated independently for more than 3 cultures with similar results.

*, $p < 0.05$ (Mann-Whitney Rank Sum non-parametric tests, two-sides).

Supplementary figure 8

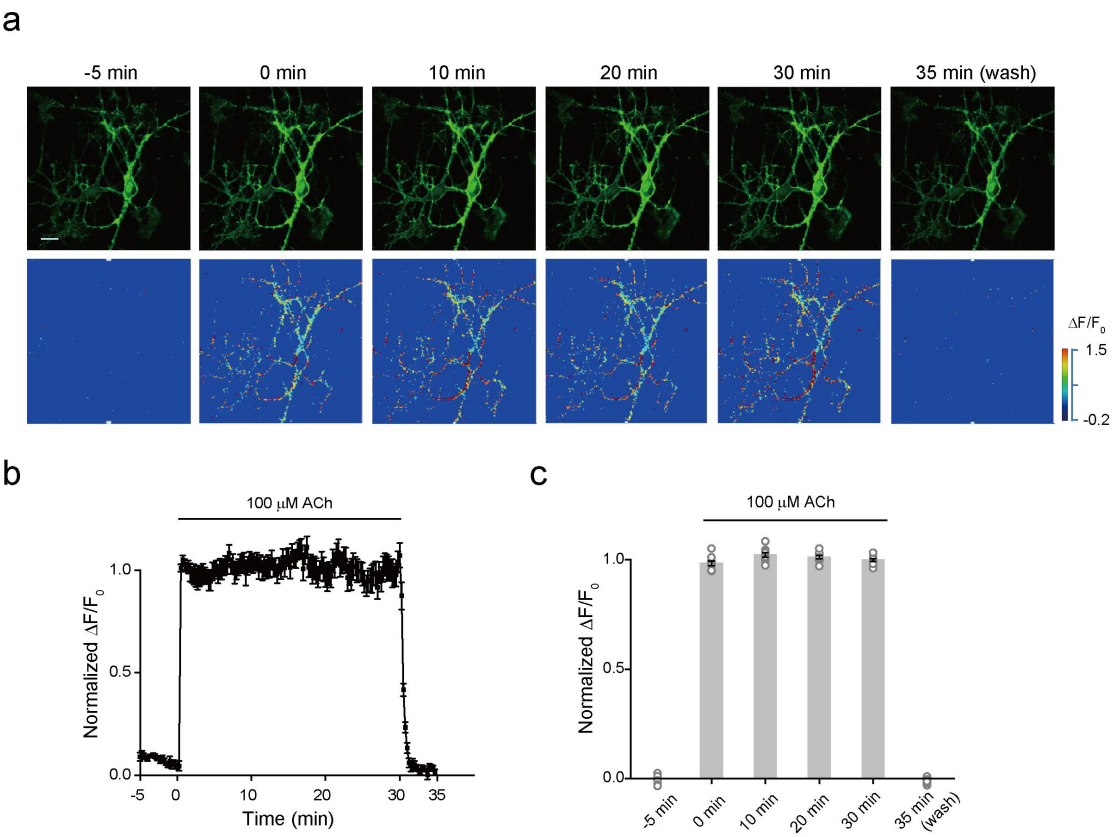

Supplementary figure 8: GACh2.0 exhibits no agonist-induced internalization in cultured cortical neurons.

(**a**) Images show a GACh2.0 expressing cultured neuron to long-term application of 100 μM ACh.

(**b**) $\Delta F/F_0$ of the GACh2.0 expressing cultured neuron to long-term application of ACh (averaged from 3 repeated trials).

(**c**) Values for GACh2.0 expressing cultured neuron at the different times (n = 9 neurons from 9 cultures, 0 min: 98.62 ± 1.01%, U = 81, p = 4.66E-5; 10 min: 100.02 ± 0.83%, U = 81, p = 4.66E-5; 20 min: 101.65 ± 0.83%, U = 81, p = 4.66E-5; 30 min: 100.37 ± 0.66%, U = 81, p = 4.66E-5; Washout: -0.70 ± 1.26%, U = 47.5, p = 0.57) after application of ACh compared with 5 min before the application (-5 min: -0.16 ±

0.27%). Values and standard errors were normalized to the averaged $\Delta F/F_0$ in ACh application.

Data are shown with mean ± s.e.m, with error bars indicate s.e.m.

Experiments in (**a**) were repeated independently for 9 cultures with similar results.

***, $p < 0.001$; n.s., not significant (Mann-Whitney Rank Sum non-parametric tests, two-sides).

Supplementary figure 9

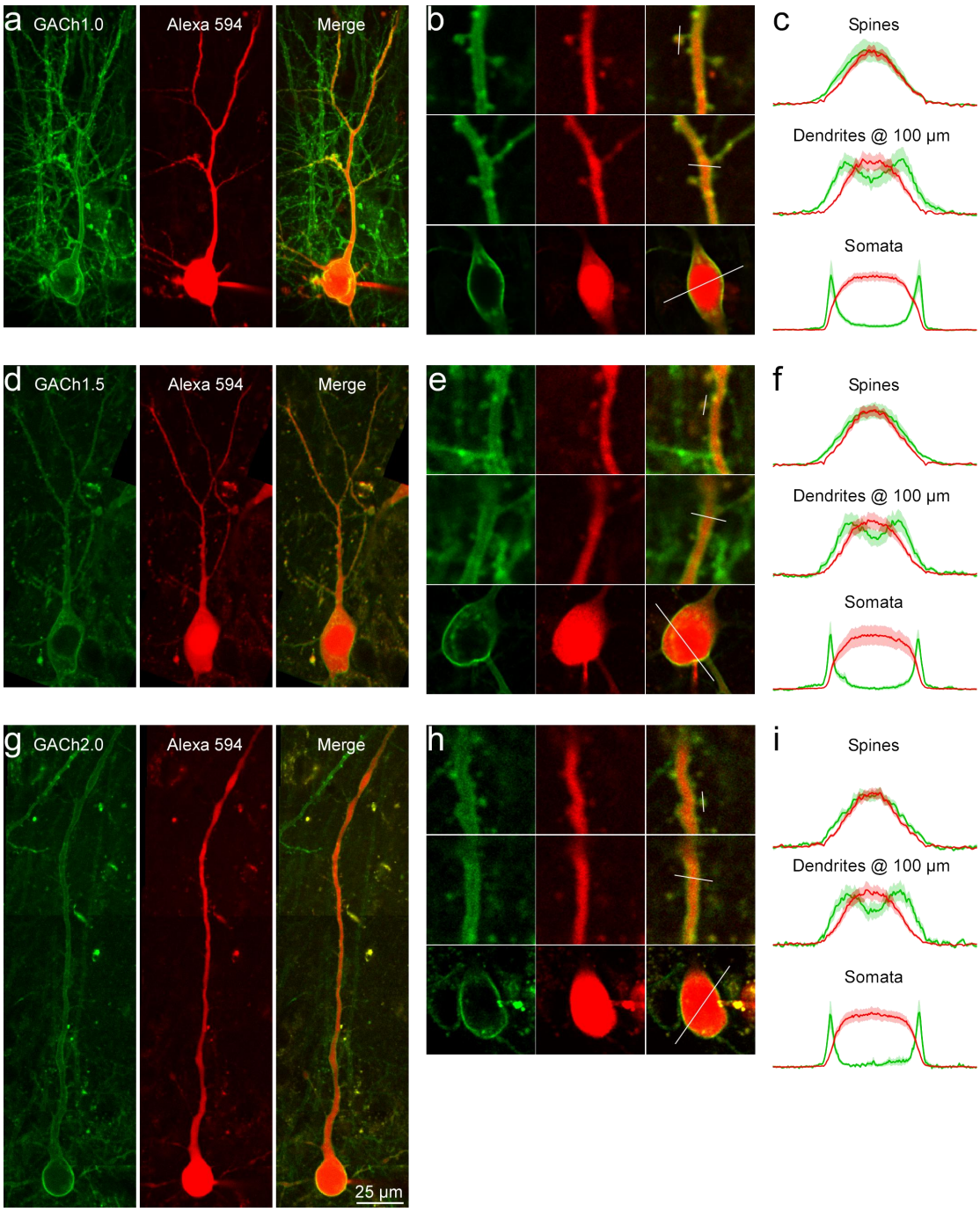

Supplementary figure 9: GACh sensors incorporate into the membrane surface of CA1 neurons.

(**a**) Thin section two-photon images (green EGFP channel, red Alexa 594 channel and overlay) of a GACh1.0 expressing CA1 neuron loaded with 20 μM Alexa 594.

(**b**) Two-photon images (green EGFP channel, red Alexa 594 channel and overlay) of the areas, in which line scanning images crossing a dendritic spine, the dendrite 100 μm away from the soma, and the soma of another GACh1.0 expressing CA1 neuron were taken.

(**c**) The averages and shaded error bands of normalized EGFP and Alexa 594 fluorescence measured with the line scanning crossing somata (*n* = 11 from 11 neurons of 6 animals), mid dendrites (at ~100 μm away from the soma; *n* = 11 from 11 neurons of 6 animals), and spines (*n* = 32 from 11 neurons of 6 animals) of CA1 neurons.

(**d**) Thin section two-photon images (green EGFP channel, red Alexa 594 channel and overlay) of a GACh1.5 expressing CA1 neuron loaded with 20 μM Alexa 594.

(**e**) Two-photon images (green EGFP channel, red Alexa 594 channel and overlay) of the areas, in which line scanning images crossing a dendritic spine, the dendrite 100 μm away from the soma, and the soma of another GACh1.5 expressing CA1 neuron were taken.

(**f**) The averages and shaded error bands of normalized EGFP and Alexa 594 fluorescence measured with the line scanning crossing somata (*n* = 12 from 12 neurons of 6 animals), mid dendrites (at ~100 μm away from the soma; *n* = 12 from 12 neurons of 6 animals), and spines (*n* = 26 from 9 neurons of 5 animals) of CA1 neurons.

(**g**) Thin section two-photon images (green EGFP channel, red Alexa 594 channel and overlay) of a GACh2.0 expressing CA1 neuron loaded with 20 μM Alexa 594. The scale bar applies to (**a**), (**d**) and (**g**).

(**h**) Two-photon images (green EGFP channel, red Alexa 594 channel and overlay) of the areas, in which line scanning images crossing a dendritic spine, the dendrite 100 μm away from the soma, and the soma of another GACh2.0 expressing CA1 neuron were taken.

(**i**) The averages and shaded error bands of EGFP and Alexa 594 fluorescence measured with the line scanning crossing somata (*n* = 11 from 11 neurons of 6 animals), mid dendrites (at ~100 μm away from the soma; *n* = 11 from 11 neurons of 6 animals), and spines (*n* = 24 from 9 neurons of 5 animals) of CA1 neurons. Data are shown with mean ± s.e.m, with shaded bands indicate the s.e.m.

Experiments in (**a**),(**b**),(**d**),(**e**),(**g**),(**h**) were repeated independently for 6 animals with similar results.

Supplementary figure 10

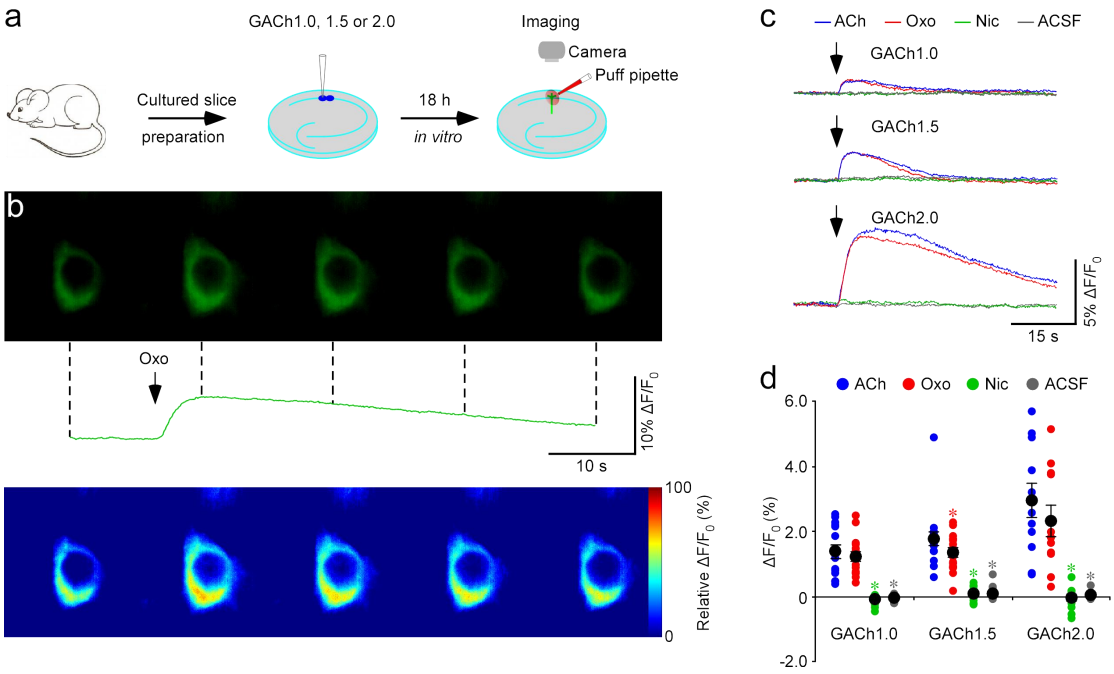

Supplementary figure 10: GACh sensors selectively respond to muscarinic agonists in brain slices.

(**a**) Schematic drawing outlines the design of imaging experiments in CA1 pyramidal neurons in cultured mouse hippocampal slices.

(**b**) Snapshots of fluorescence response of a GACh2.0 expressing CA1 neuron to a brief application (500 ms) of 10 mM cholinergic agonist oxotremorine (Oxo).

(**c**) Fluorescence responses of GACh1.0, GACh1.5 and GACh2.0 expressing CA1 neurons to a brief puff (500 ms) of 100 mM acetylcholine (ACh), 10 mM oxotremorine (Oxo), 10 mM nicotine (Nic) and ACSF.

(**d**) Values for the fluorescence responses of GACh1.0, GACh1.5 and GACh2.0 expressing CA1 neurons to the application of Oxo (GACh1.0: 1.39 ± 0.20%, Z = -1.250, p = 0.21, n = 15 neurons from 8 animals; GACh1.5: 1.75 ± 0.22%, Z = -3.006,

p = 0.003, n = 17 neurons from 8 animals; GACh2.0: 2.91 ± 0.52%, Z = -1.423, p = 0.16, n = 11 neurons from 8 animals), Nic (GACh1.0: -0.09 ± 0.03%, Z = -3.408, p = 0.001, n = 15 neurons from 8 animals; GACh1.5: 0.06 ± 0.04%, Z = -3.622, p = 0.0005, n = 17 neurons from 8 animals; GACh2.0: -0.06 ± 0.11%, Z = -2.934, p = 0.003, n = 11 neurons from 8 animals) and ACSF (GACh1.0: -0.04 ± 0.02%, Z = -3.408, p = 0.0005, n = 15 neurons from 8 animals; GACh1.5: 0.10 ± 0.04%, Z = -3.622, p = 0.0005, n = 17 neurons from 8 animals; GACh2.0: 0.05 ± 0.04%, Z = -2.934, p = 0.003, n = 11 neurons from 8 animals) compared to ACh (GACh1.0: 1.20 ± 0.15%, n = 15 neurons from 8 animals; GACh1.5: 1.31 ± 0.13%, n = 17 neurons from 8 animals; GACh2.0: 2.31 ± 0.47%, n = 11 neurons from 8 animals). Note no ACSF- and Nicotine-induced signal, verifying the puffing system.

Data are shown with mean ± s.e.m, with large black dots indicate mean responses, error bars indicate s.e.m.

Experiments in (**b**),(**c**) were repeated independently for 8 animals with similar results.

*, $p < 0.05$ (Wilcoxon tests, two-sides).

Supplementary figure 11

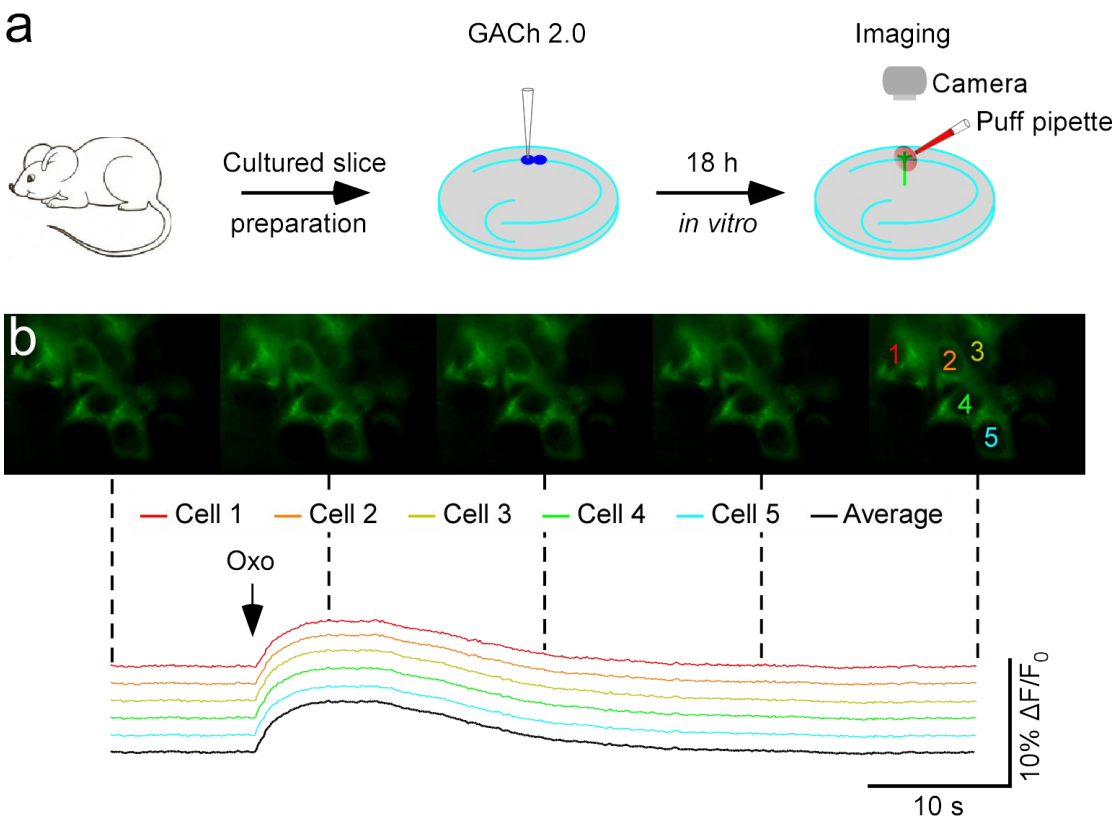

Supplementary figure 11: Multiple GACh expressing neurons respond to muscarinic agonists simultaneously.

(**a**) Schematic drawing outlines the design of imaging experiments in CA1 pyramidal neurons in cultured mouse hippocampal slices.

(**b**) Snapshots of fluorescence responses of five GACh2.0 expressing CA1 neurons to a brief application (500 ms) of 10 mM cholinergic agonist oxotremorine (Oxo). Note the synchronic responses in multiple GACh2.0 expressing CA1 neurons.

Experiments in (**b**) were repeated independently for 8 animals with similar results.

Supplementary figure 12

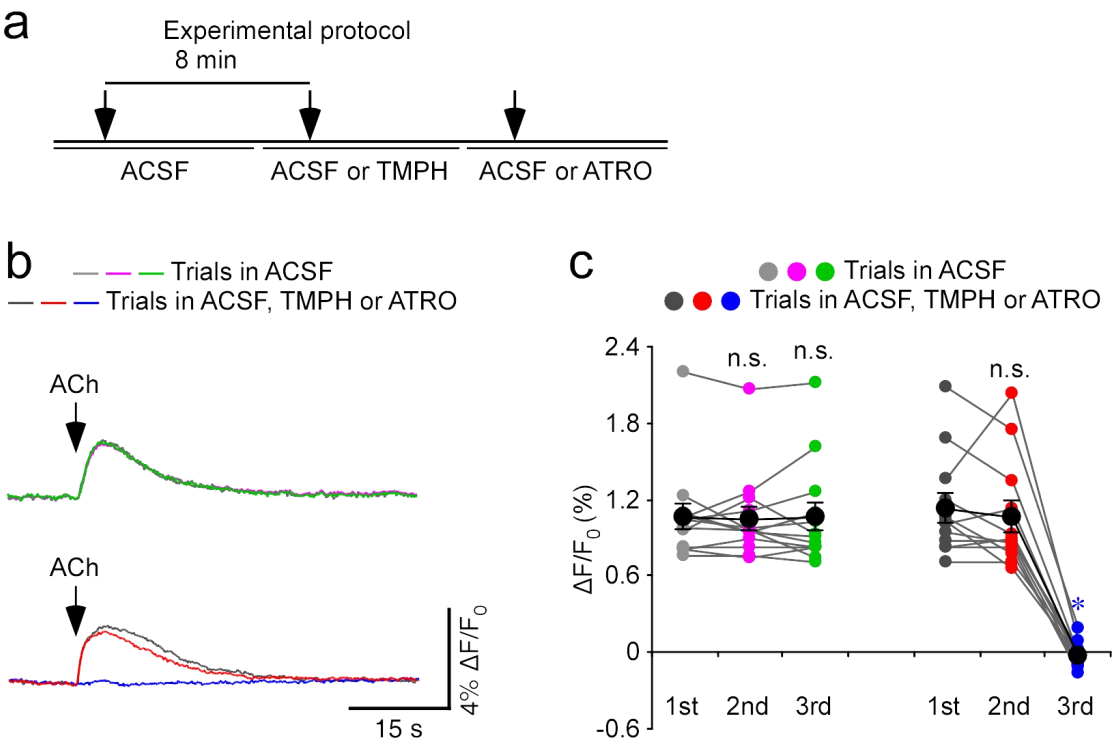

Supplementary figure 12: GACh sensors detect ACh as muscarinic receptors in brain slices.

(**a**) Agonist puff stimulation protocol for pharmacology experiments.

(**b**) Fluorescence responses of GACh2.0 expressing mouse CA1 pyramidal neurons to repetitive puffs (500 ms) of 100 mM acetylcholine (ACh) in normal ACSF, ACSF containing 1 µM 2,2,6,6-tetramethylpiperidin-4-yl heptanoate (TMPH) or 1 µM atropine (ATRO).

(**c**) Values for the fluorescence responses of GACh2.0 expressing CA1 pyramidal neurons to applications of ACh in normal ACSF in the 2nd and 3rd trials (2nd trial: 1.05 ± 0.09%, Z = -0.454, p = 0.65; 3rd trial: 1.06 ± 0.11%, Z = -0.756, p = 0.45) compared to that in the 1st trial (1st ACSF: 1.07 ± 0.10%; n = 13 neurons from 6 animals), and

those in ACSF with antagonists in the 2nd and 3rd trials (TMPH: 1.06 ± 0.12%, Z = -1.021, p = 0.31; ATRO: -0.02 ± 0.03%, Z = -3.059, p = 0.002) compared to that in normal ACSF in the 1st trial (1st ACSF: 1.13 ± 0.12%; n = 12 neurons from 7 animals). Data are shown with mean ± s.e.m, with large black dots indicate mean responses, error bars indicate s.e.m.

Experiments in (**b**) were repeated independently for more than 6 animals with similar results.

*, $p < 0.05$ (Wilcoxon tests, two-sides).

Supplementary figure 13

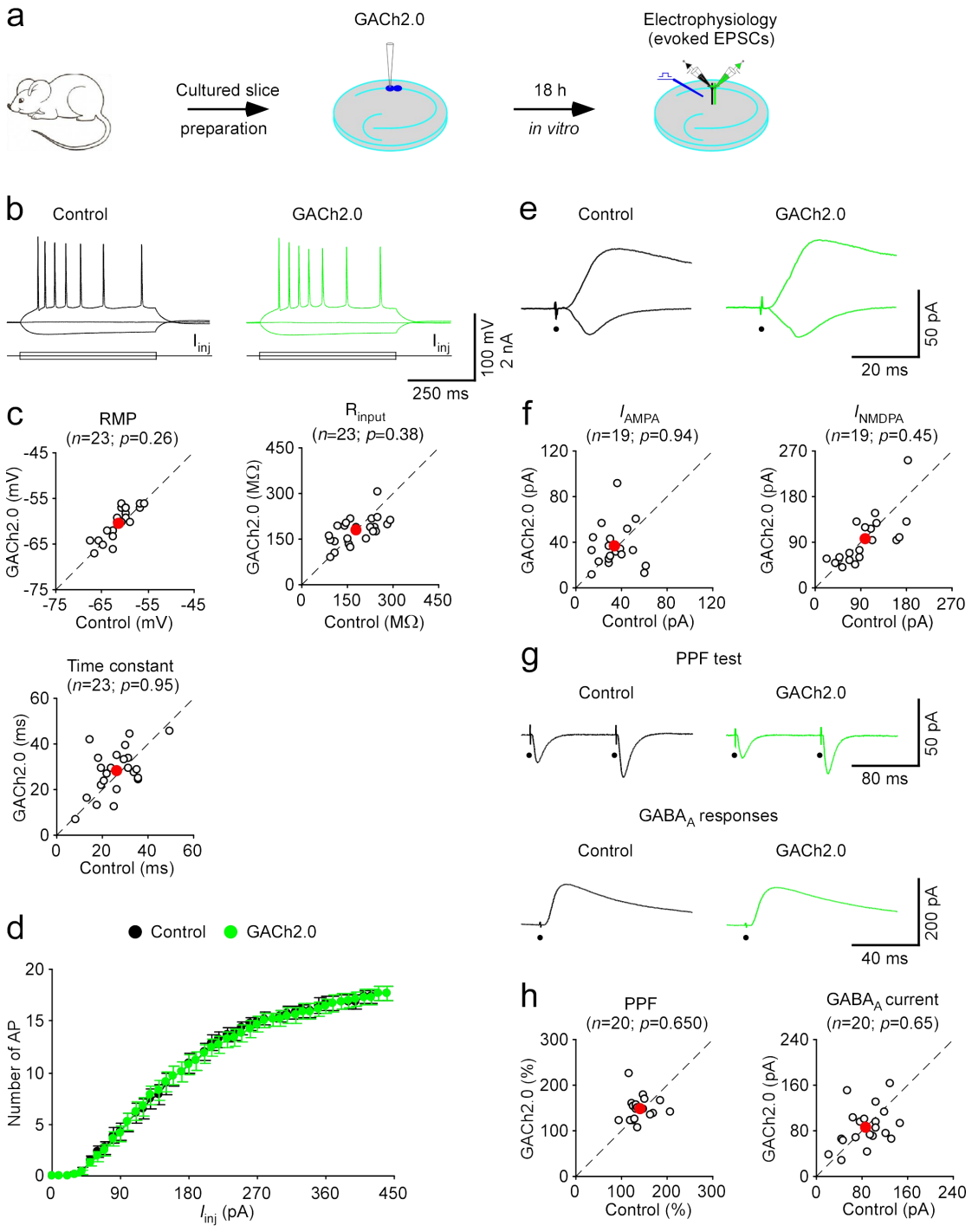

Supplementary figure 13: GACh sensors have no effect on basic membrane and synaptic properties.

(**a**) Schematic drawing outlines the design of electrophysiology experiments in CA1 pyramidal neurons in cultured mouse hippocampal slices.

(**b**) Evoked responses to step depolarizing and hyperpolarizing pulses recorded from neighboring non-expressing (Ctrl) and GACh2.0 expressing CA1 neurons.

(**c**) Values for resting membrane potentials (Ctrl: -60.7 ± 0.6 mV; Exp: -60.3 ± 0.7 mV; n = 23 neurons from 12 animals; Z = -1.234, p = 0.26), time constants (Ctrl: 27.2 ± 1.9 ms; Exp: 27.9 ± 2.1 ms; n = 23 neurons from 12 animals; Z = 0.061, p = 0.95), and input resistances (Ctrl: 189.4 ± 13.4 MΩ; Exp: 180.5 ± 9.6 MΩ; n = 23 neurons from 12 animals; Z = -0.882, p = 0.38) in neighboring non-expressing (Ctrl) and GACh2.0 expressing neurons.

(**d**) The numbers of action potentials evoked by 500-ms depolarizing current injections in GACh2.0 expressing and control non-expressing CA1 neurons are plotted against the intensity of injecting depolarizing currents (n = 23 neurons from 12 animals).

(**e**) Evoked AMPA-R- (-60 mV) and NMDA-R- (+40 mV) mediated responses recorded from neighboring control non-expressing (Ctrl) and GACh2.0 expressing CA1 pyramidal neurons.

(**f**) Values for AMPA (Ctrl: -36.6 ± 3.4 pA; Exp: -37.0 ± 4.4 pA; n = 19 neurons from 12 animals; Z = 0.080, p = 0.98) and NMDA (Ctrl: 104.7 ± 10.8 pA; Exp: 97.9 ± 11.6 pA; n = 19 neurons from 12 animals; Z = -0.765, p = 0.45) responses in CA1 neurons expressing GACh2.0.

(**g**) Evoked AMPA-R- (-60 mV) and GABA-R- (0 mV) mediated responses recorded from neighboring non-expressing (Ctrl) and GACh2.0 expressing CA1 pyramidal neurons.

(**h**) Ratios of paired-pulses facilitation (PPF) (Ctrl: 145.5 ± 5.8%; Exp: 149.7 ± 5.9%; n = 20 neurons from 12 animals; Z = 0.523, p = 0.60) and synaptic GABA responses (Ctrl: 88.0 ± 7.7 pA; Exp 85.4 ± 7.8 pA; n = 20 neurons from 3 animals; Z = -0.448, p = 0.65) in GACh2.0 expressing neurons are plotted against those obtained from control non-expressing neurons.

Data are shown with mean ± s.e.m, with error bars indicate s.e.m.

Wilcoxon tests performed, two-sides.

Supplementary figure 14

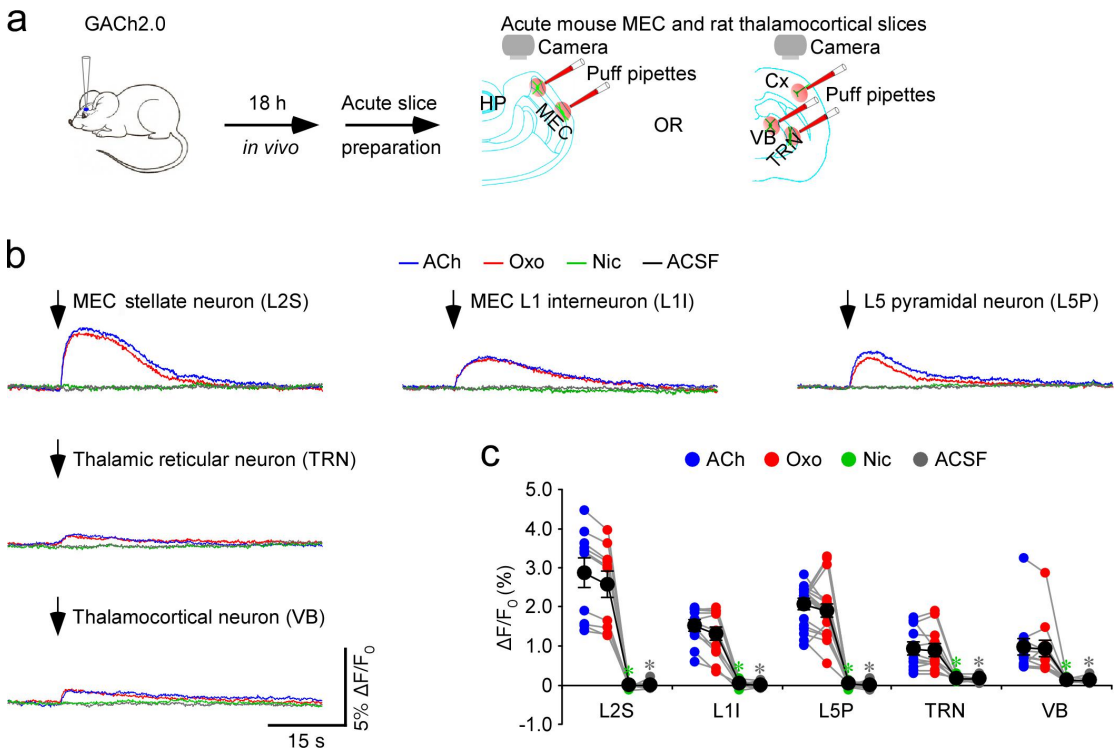

Supplementary figure 14: GACh2.0 selectively responds to muscarinic agonists in various brain regions.

(**a**) Schematic drawing outlines the design of imaging experiments using various *in vivo* viral expression and *in vitro* acute mouse and rat slice preparations. Cx: cortex; HP: hippocampus; MEC: medial entorhinal cortex; TRN: thalamic reticular nucleus; VB: ventral basal nucleus.

(**b**) Fluorescence responses of GACh2.0 expressing MEC L2 stellate neuron (L2S), MEC L1 interneuron (L1I) and cortical L5 pyramidal neuron (L5P) of mice, and thalamic reticular neuron (TRN), and thalamocortical neuron in the ventral basal nucleus (VB) of rats to a 500-ms puff of 100 mM acetylcholine (ACh), 10 mM oxotremorine (Oxo), 10 mM nicotine (Nic) and ACSF.

(**c**) Values for the fluorescence responses of GACh2.0 expressing L2S, L1I, L5P, TRN and VB neurons to the application of Oxo (L2S: 2.54 ± 0.34%, Z = -2.803, p = 0.005, n = 10 neurons from 4 animals; L1I: 1.29 ± 0.19%, Z = -2.223, p = 0.026, n = 11 neurons from 5 animals; L5P: 1.95 ± 0.17%, Z = -0.936, p = 0.35, n = 19 neurons from 6 animals; TRN: 0.87 ± 0.15%, Z = -0.078, p = 0.94, n = 12 neurons from 5 animals; VB: 0.91 ± 0.20%, Z = -1.412, p = 0.16, n = 12 neurons from 3 animals), Nic (L2S: 0.04 ± 0.02%, Z = -2.803, p = 0.005, n = 10 neurons from 4 animals; L1I: 0.03 ± 0.03%, Z = -2.934, p = 0.003, n = 11 neurons from 5 animals; L5P: -0.01 ± 0.02%, Z = -3.382, p = 0.005, n = 19 neurons from 6 animals; TRN: 0.15 ± 0.02%, Z = -3.059, p = 0.002, n = 12 neurons from 5 animals; VB: 0.11 ± 0.01%, Z = -3.059, p = 0.002, n = 12 neurons from 3 animals), and ACSF (L2S: -0.02 ± 0.03%, Z = -2.803, p = 0.003, n = 10 neurons from 4 animals; L1I: -0.02 ± 0.02%, Z = -2.934, p = 0.0005, n = 11 neurons from 5 animals; L5P: -0.01 ± 0.02%, Z = -3.382, p = 0.0005, n = 19 neurons from 6 animals; TRN: 0.14 ± 0.02%, Z = -3.059, p = 0.002, n = 12 neurons from 5 animals; VB: -0.10 ± 0.02%, Z = -3.059, p = 0.002, n = 12 neurons from 3 animals) compared to application of ACh (MEC-L2S: 2.84 ± 0.36%; MEC-L1I: 1.47 ± 0.13%; L5P: 2.02 ± 0.13%; TRN: 0.91 ± 0.15%; VB: 0.95 ± 0.21%).

Data are shown with mean ± s.e.m, with large black dots indicate mean responses, error bars indicate s.e.m.

*, p < 0.05 (Wilcoxon tests, two-sides).

Supplementary figure 15

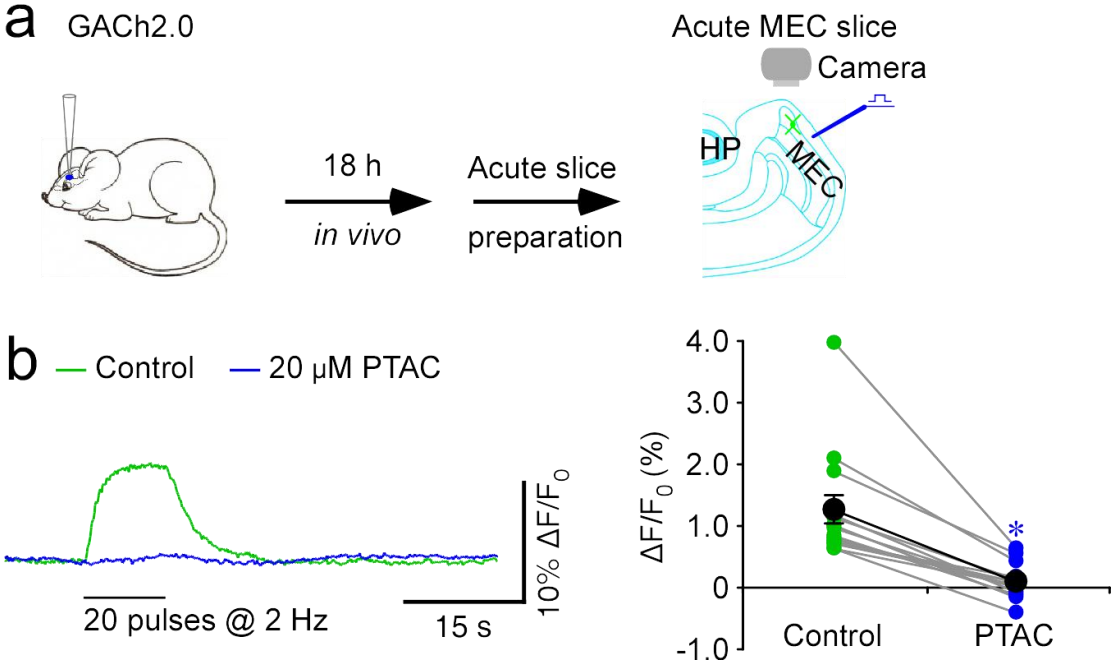

Supplementary figure 15: The specificity of GACh2.0 in detecting cholinergic transmission.

(**a**) Schematic drawing outlines the design of stimulation-imaging experiments using an *in vivo* viral expression and *in vitro* mouse entorhinal brain slice preparation. HP: hippocampus; MEC: medial entorhinal cortex**.**

(**b**) Left, fluorescence responses of a GACh2.0 expressing MEC stellate neuron to layer 1 electrical stimulation in the normal bath solution, in bath solution containing 20 μM (5*R*,6*R*)6-(3-propylthio-1,2,5-thiadiazol-4-yl)-1-azabicyclooctane (PTAC). Right, values for the fluorescence responses of GACh2.0 MEC stellate neurons to layer 1 electrical stimulation in the bath containing 20 μM PTAC compared to those in the normal bath solution (Ctrl: 1.23 ± 0.24%; Exp: 0.09 ± 0.07%, Z = -3.296; p = 0.001; n = 14 neurons from 9 animals).

Data are shown with mean ± s.e.m, with large black dots indicate mean responses, error bars indicate s.e.m.

*, $p < 0.05$ (Wilcoxon tests, two-sides).

Supplementary figure 16

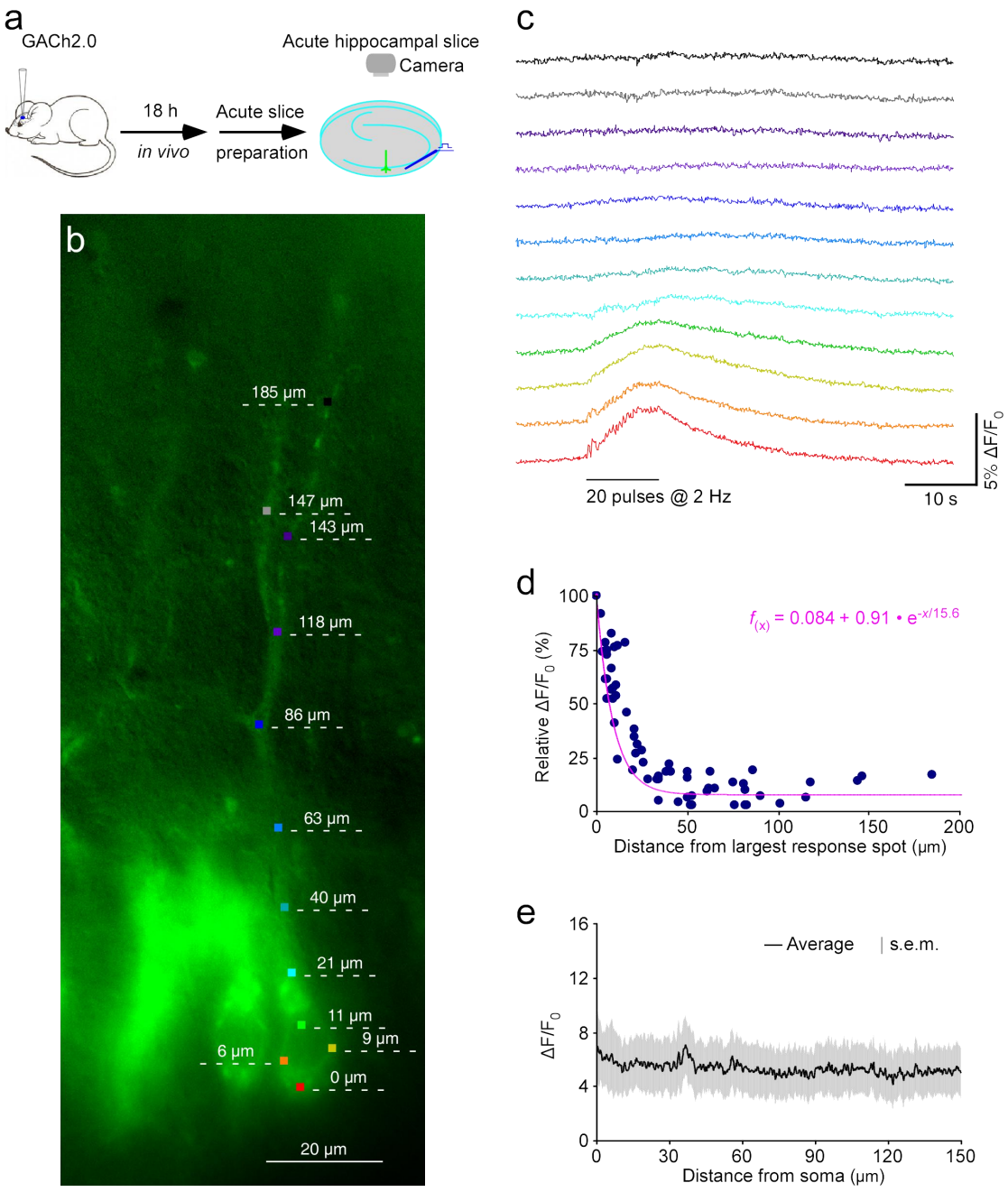

Supplementary figure 16: GACh2.0 maps somatodendritic cholinergic signals in the hippocampus.

(**a**) Schematic drawing outlines the design of stimulation-imaging experiments using an *in vivo* viral expression and *in vitro* acute mouse hippocampal slice preparation**.**

(**b**) Snapshot of fluorescent image of GACh2.0 expressing CA1 pyramidal neurons.

(**c**) Minimal electrical stimuli applied in the stratum oriens induced different fluorescence responses in subcellular regions of interest (ROIs), marked by color squares (~1.5 μm x ~1.5 μm) in (**b**), along the somatodendritic axis of a GACh2.0 expressing CA1 neuron.

(**d**) Plot of $\Delta F/F_0$ responses against the distance from the ROI with the largest $\Delta F/ F_0$. The data points (*n* = 70 from 10 neurons of 6 animals) were arbitrarily fitted with a single exponential decay function (pink line), resulting in an estimated volume spread length constant of ~15 μm. Note that the relative $\Delta F/F_0$ responses, or the $\Delta F/F_0$ responses normalized to the largest $\Delta F/F_0$ responses in the same neurons, were used in analysis.

(**e**) $\Delta F/F_0$ responses mapped along the entire somatodendritic axis of expressing CA1 neurons indicate no dependence on locations of ROIs (*n* = 11 neurons from 5 animals).

Data are shown with mean ± s.e.m, with shaded bands indicate the s.e.m.

Experiments in (**b**) were repeated independently for more than 5 animals with similar results.

Supplementary figure 17

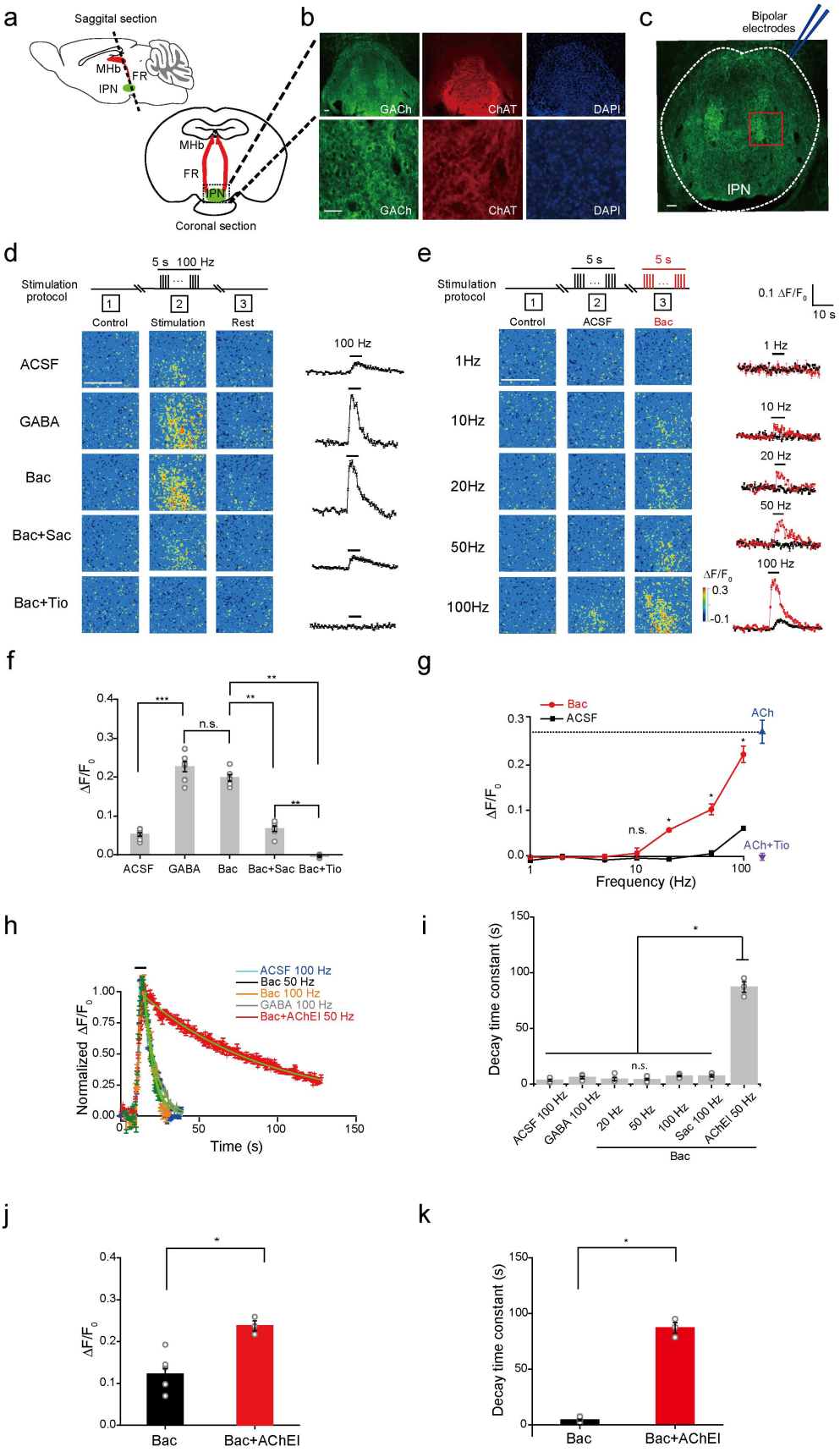

Supplementary figure 17: GACh2.0 shows frequency- and $GABA_BR$-dependent ACh release in lPN.

(**a**) Schematic drawings show the preparation of MHb-fr-lPN slices preserving the medial habenula (MHb), the fasciculus retroflexus (fr, red) and interpeduncular nucleus (lPN, green).

(**b**) Immunostaining shows expression of GACh2.0 (green) in lPN neurons and ChAT in habenula cholinergic axonal terminals. DAPI staining (blue) were used to label the cell nuclei.

(**c**) Image shows the location of a bipolar electrode used to stimulate MHb efferent fibers.

(**d**) Two-photon imaging of ACh dynamics in lPN. Electrical stimulation at 100 Hz for 5 s elicited a modest ACh release (ACSF, peak $\Delta F/F_0$ 4.37 ± 0.72%). Bath application of GABA (1 μM) or baclofen (Bac, 2 μM), a specific $GABA_B$ receptor agonist, markedly potentiated the fluorescence responses (GABA: peak $\Delta F/F_0$ 23.08 ± 0.46%; Bac: peak $\Delta F/F_0$ 25.12 ± 0.64%). The potentiated signals were blocked by 2-hydroxy-saclofen (Sac, 100 μM), a specific $GABA_B$ receptor antagonist (Bac+Sac, peak $\Delta F/F_0$ 5.20 ± 0.87%). Tio (10 μM) completely abolished the evoked fluorescence increase (Bac+Tio: peak $\Delta F/F_0$ 0.27 ± 0.38%). A selected square (170 μm × 170 μm) was sampled at 2.3 Hz with 25 ROIs (4 μm × 4 μm, each) selected for analysis.

(**e**) Frequency-dependent potentiation of cholinergic release by the $GABA_B$ receptor in lPN. Similar as in (**d**), with the stimulation frequencies varied from 1 Hz to 100 Hz. ACSF 1 Hz, peak $\Delta F/F_0$ 0.54 ± 0.11%, Bac 1 Hz, peak $\Delta F/F_0$ 0.19 ± 0.47%. ACSF 10

Hz, peak $\Delta F/F_0$ 0.22 ± 0.09%, Bac 10 Hz, peak $\Delta F/F_0$ 4.67 ± 1.21%. ACSF 20 Hz, peak $\Delta F/F_0$ 0.44 ± 0.42%, Bac 20 Hz, peak $\Delta F/F_0$ 7.41 ± 0.58%. ACSF 50 Hz, peak $\Delta F/F_0$ 0.65 ± 0.43%, Bac 50 Hz, peak $\Delta F/F_0$ 11.13 ± 0.19%. ACSF 100 Hz, peak $\Delta F/F_0$ 4.37 ± 0.72%, Bac 100 Hz, peak $\Delta F/F_0$ 25.12 ± 0.64%.

(**f,g**) Group data of presynaptic potentiation by $GABA_B$ receptors. ACSF: $\Delta F/F_0$ 3.73 ± 1.16%, *n* = 8 slices from 8 mice, GABA: $\Delta F/F_0$ 23.08 ± 0.64%, *n* = 8 slices from 8 mice, Bac: $\Delta F/F_0$ 25.16 ± 2.95%, *n* = 6 slices from 6 mice, Bac+Sac: $\Delta F/F_0$ 5.51 ± 1.27%, *n* = 6 slices from 6 mice, Bac+Tio: $\Delta F/F_0$ 0.16 ± 0.80%, *n* = 5 slices from 5 mice. *U* = 33, *p* = 0.10 for GABA and Bac. *U* = 64, *p* = 9,39E-4 for ACSF and GABA. *U* = 36, *p* = 0.005 for Bac and Bac+Sac. *U* = 30, *p* = 0.008 for Bac and Bac+Tio. *U* = 30, *p* = 0.008 for Bac+Sac and Bac+Tio. *N* = 5 slices in (**g**) are averaged. ACSF: 1 Hz, $\Delta F/F_0$ −1.05 ± 0.44%, Bac: 1 Hz, $\Delta F/F_0$ -0.36 ± 0.29%. ACSF: 2 Hz, $\Delta F/F_0$ −0.23 ± 0.51%, Bac: 2 Hz, $\Delta F/F_0$ −0.45 ± 0.17%. ACSF: 5 Hz, $\Delta F/F_0$ -0.97 ± 0.27%, Bac: 5 Hz, $\Delta F/F_0$ −0.26 ± 0.57%. ACSF: 10 Hz, $\Delta F/F_0$ −0.53 ± 0.41%, Bac: 10 Hz, $\Delta F/F_0$ 0.55 ± 0.37%. ACSF: 20 Hz, $\Delta F/F_0$ −0.76 ± 0.34%, Bac: 20 Hz, $\Delta F/F_0$ 5.65 ± 0.37%. ACSF: 50 Hz, $\Delta F/F_0$ 0.42 ± 0.64%, Bac: 50 Hz, $\Delta F/F_0$ 10.18 ± 1.21%. ACSF: 100 Hz, $\Delta F/F_0$ 6.00 ± 0.32%, Bac: 100 Hz, $\Delta F/F_0$ 22.32 ± 1.81%. With baclofen treatment, 10 Hz: *U* = 14, *p* = 0.83; 20 Hz: *U* = 25, *p* = 0.011; 50 Hz: *U* = 25, *p* = 0.012; 100 Hz: *U* = 25, *p* = 0.012 compared with the same frequency stimulation in ACSF groups.

(**h,i**) Kinetics of ACh dynamics probed by GACh2.0. The evoked fluorescence responses in different stimulation conditions were normalized to compare their kinetics. AChEI treatment (donepezil, 2 μM) significantly prolonged the decay kinetics

comparing with the rest of the groups (ACSF 100 Hz: 4.46 ± 1.48 s, GABA 100 Hz: 6.67 ± 1.23 s, Bac 20 Hz: 5.31 ± 2.29 s, Bac 50 Hz: 4.24 ± 0.75 s, Bac 100 Hz: 7.43 ± 0.59 s. Bac+Sac 100 Hz: 6.68 ± 0.74 s, Bac+AChEI 50 Hz: 89.6 ± 9.89 s). $U = 15$, $p = 0.037$ for ACSF 100 Hz, $U = 15$, $p = 0.037$ for GABA 100 Hz, $U = 15$, $p = 0.037$ for Bac 20 Hz, $U = 27$, $p = 0.016$ for Bac 50 Hz, $U = 18$, $p = 0.028$ for Bac 100 Hz, $U = 15$, $p = 0.037$ for Bac+Sac 100 Hz, compared with Bac+AChEI 50 Hz group.

(**j,k**) The peak fluorescence response and decay time constant before and after donepezil application ($\Delta F/F_0$ 15.7 ± 1.8%, $n = 8$ slices from 8 mice before donepezil vs. 23.8 ± 1.2%, $n = 3$ slices of 3 mice after donepezil, $U = 24$, $p = 0.019$. Time constant = 3.88 ± 0.74 s, $n = 8$ slices from 8 mice before donepezil, vs. 89.6 ± 9.89 s, $n = 3$ slices of 3 mice after donepezil, $U = 24$, $p = 0.016$).

Fluorescence response and time constant were calculated by averaging 20-30 ROIs from each slice.

Data are shown with mean ± s.e.m, with error bars indicate s.e.m.

Experiments in (**b**),(**d**),(**e**) were repeated independently for more than 3 animals with similar results.

*, $p < 0.05$; **, $p < 0.01$, ***; $p < 0.001$; n.s., not significant (Mann-Whitney Rank Sum non-parametric tests, two-sides). All scale bars: 50 μm

Supplementary figure 18

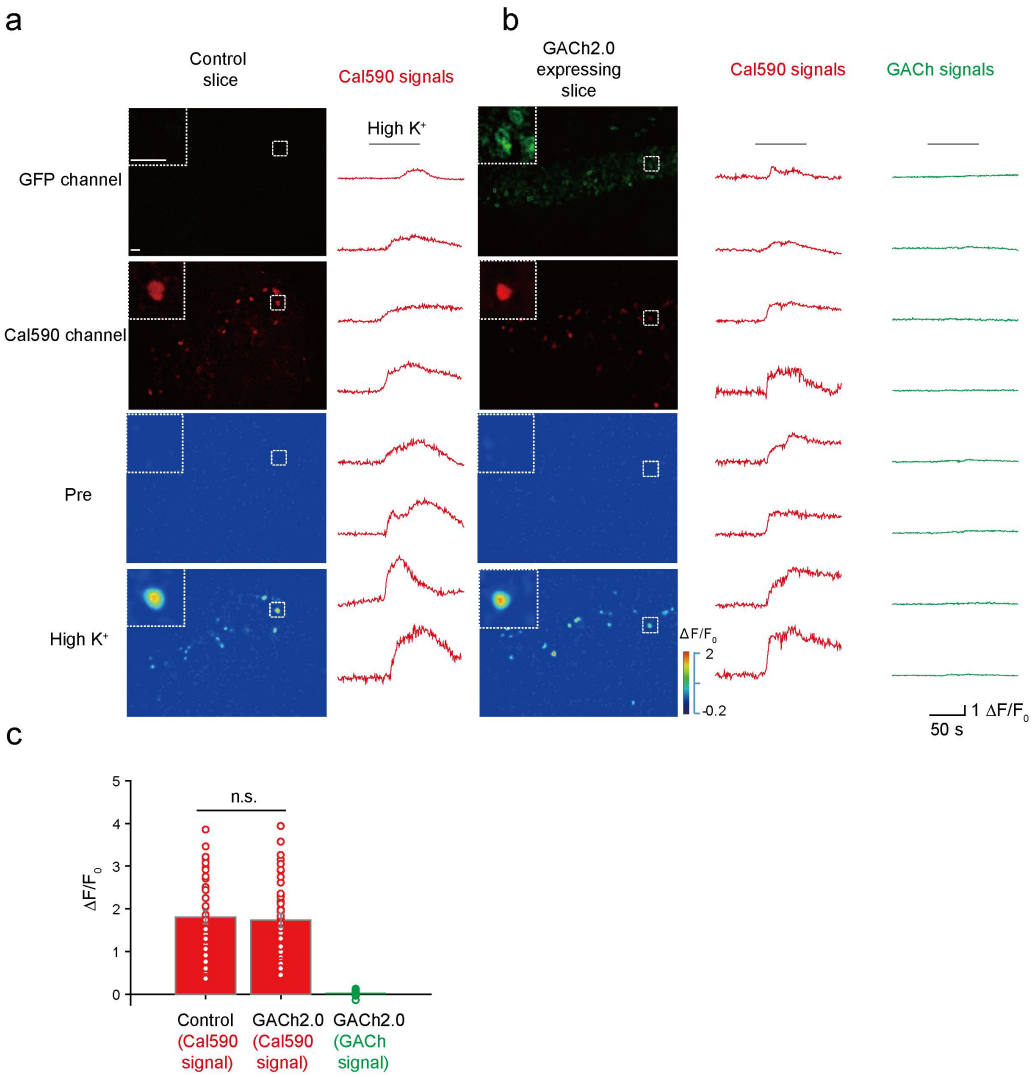

Supplementary figure 18: Chronic expression of GACh2.0 has no effect on the high K^+-induced Ca^{2+} responses in hippocampal cells.

(**a**,**b**) Representative snapshots of a control (**a**) and a GACh2.0 expressing (**b**) hippocampal slice, loaded with a red Ca^{2+} dye, Cal590. High K^+ (90 mM) application elicited reversible enhancements of Cal590 signals in individual neurons, as exemplified by traces on the right of the images. The corresponding traces of green channel in GACh2.0 expressing cells were also shown on the right.

(**c**) Quantification of Cal590 signals (Control Cal590: 1.80 ± 0.15, *n* = 53 neurons of 6 slices from 4 mice; GACh2.0 Cal590: 1.73 ± 0.17, *n* = 63 neurons of 7 slices from 4 mice, *U* = 1680, *p* = 0.96) and GACh signal (GACh2.0: 2.79 ± 0.69%, *n* = 41 neurons of 7 slices from 4 mice) to High K^+ treatment.

Slices were prepared from control non-expressing and GACh2.0 expressing mice after 40-50 day expression.

Data are shown with mean ± s.e.m, with error bars indicate s.e.m. All scale bars: 50 μm.

Experiments in (**a**),(**b**) were repeated independently for 4 animals with similar results.

n.s., not significant (Mann-Whitney Rank Sum non-parametric tests, two-sides).

Supplementary figure 19

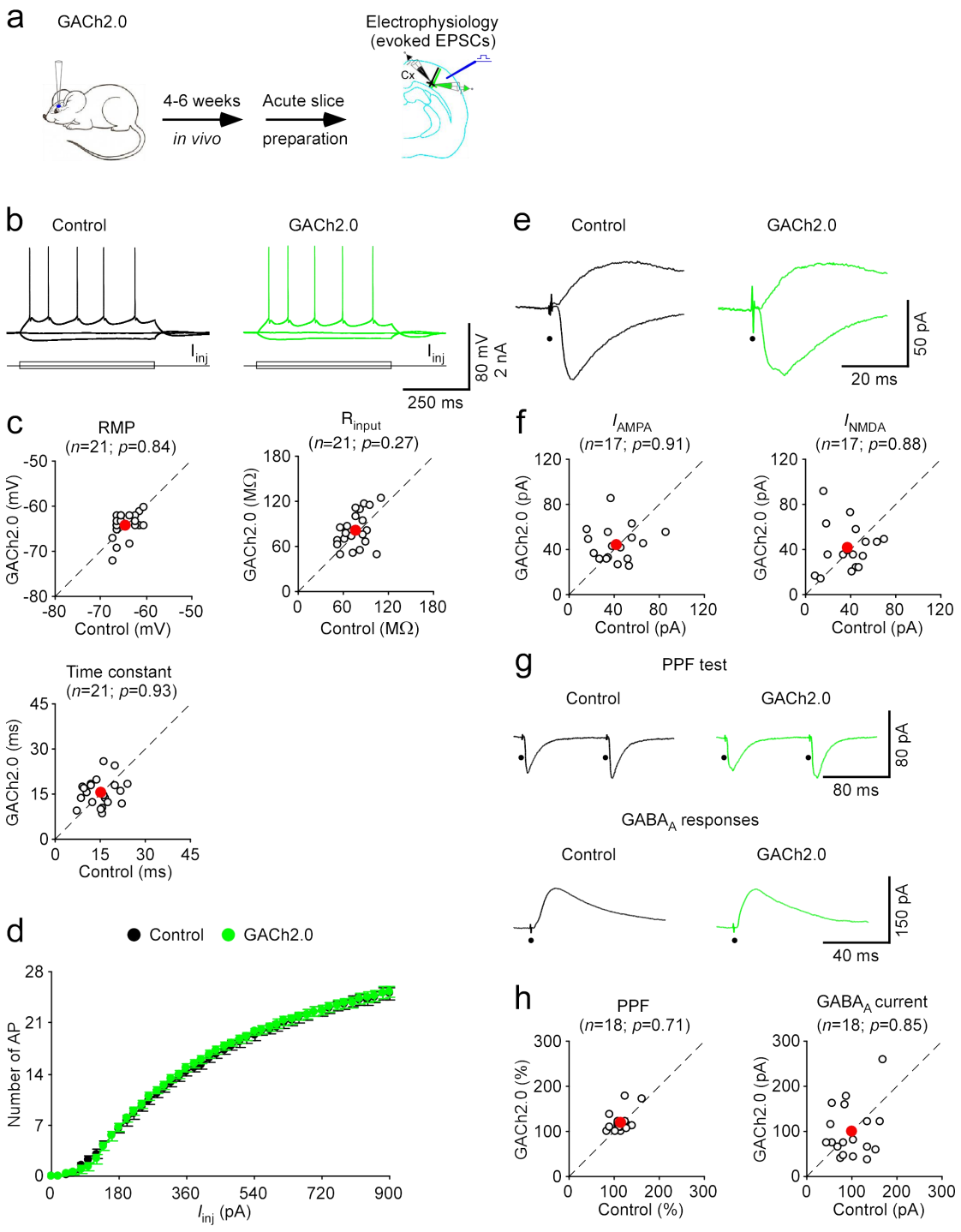

Supplementary figure 19: Chronic expression of GACh sensors *in vivo* have no effect on basic membrane and synaptic properties.

(**a**) Schematic drawing outlines the design of electrophysiology experiments using an *in vivo* viral expression and *in vitro* mouse barrel cortical slice preparation.

(**b**) Evoked responses to step depolarizing and hyperpolarizing pulses recorded from neighboring non-expressing (Ctrl) and GACh2.0 expressing layer 5 pyramidal neurons.

(**c**) Values for resting membrane potentials (Ctrl: -64.9 ± 0.5 mV; Exp: -64.0 ± 0.6 mV; n = 21 neurons from 12 animals; Z = -0.208, p = 0.84), time constants (Ctrl: 15.4 ± 1.0 ms; Exp: 15.4 ± 1.0 ms; n = 21 neurons from 12 animals; Z = 0.087, p = 0.95), and input resistances (Ctrl: 79.1 ± 3.6 MΩ; Exp: 83.2 ± 5.2 MΩ; n = 21 neurons from 12 animals; Z = 1.095, p = 0.27) in neighboring non-expressing (Ctrl) and GACh2.0 expressing neurons.

(**d**) The numbers of action potentials evoked by 500-ms depolarizing current injections in GACh2.0 expressing and control non-expressing layer 5 pyramidal neurons are plotted against the intensity of injecting depolarizing currents.

(**e**) Evoked AMPA-R- (-60 mV) and NMDA-R- (+40 mV) mediated responses recorded from neighboring control non-expressing (Ctrl) and GACh2.0 expressing layer 5 pyramidal neurons.

(**f**) Values for AMPA (Ctrl: -42.5 ± 4.4 pA; Exp: -44.4 ± 3.8 pA; n = 17 neurons from 9 animals; Z = 0.118, p = 0.91) and NMDA (Ctrl: 38.0 ± 4.2 pA; Exp: 41.2 ± 5.0 pA; n = 17 neurons from 9 animals; Z = -0.115, p = 0.88) responses in layer 5 pyramidal neurons expressing GACh2.0.

(**g**) Evoked AMPA-R- (-60 mV) and GABA-R- (0 mV) mediated responses recorded from neighboring non-expressing (Ctrl) and GACh2.0 expressing layer 5 pyramidal neurons.

(**h**) Ratios of paired-pulses facilitation (PPF) (Ctrl: 115.8 ± 4.4%; Exp: 119.2 ± 5.3%; n = 18 neurons from 9 animals; Z = 0.370, p = 0.71) and synaptic GABA responses (Ctrl: 99.4 ± 9.4 pA; Exp: 98.7 ± 14.0 pA; n = 18 neurons from 9 animals; Z = -0.196, p = 0.85) in GACh2.0 expressing neurons are plotted against those obtained from control non-expressing neurons.

Data are shown with mean ± s.e.m, with error bars indicate s.e.m.

Wilcoxon tests performed, two-sides.

Supplementary figure 20

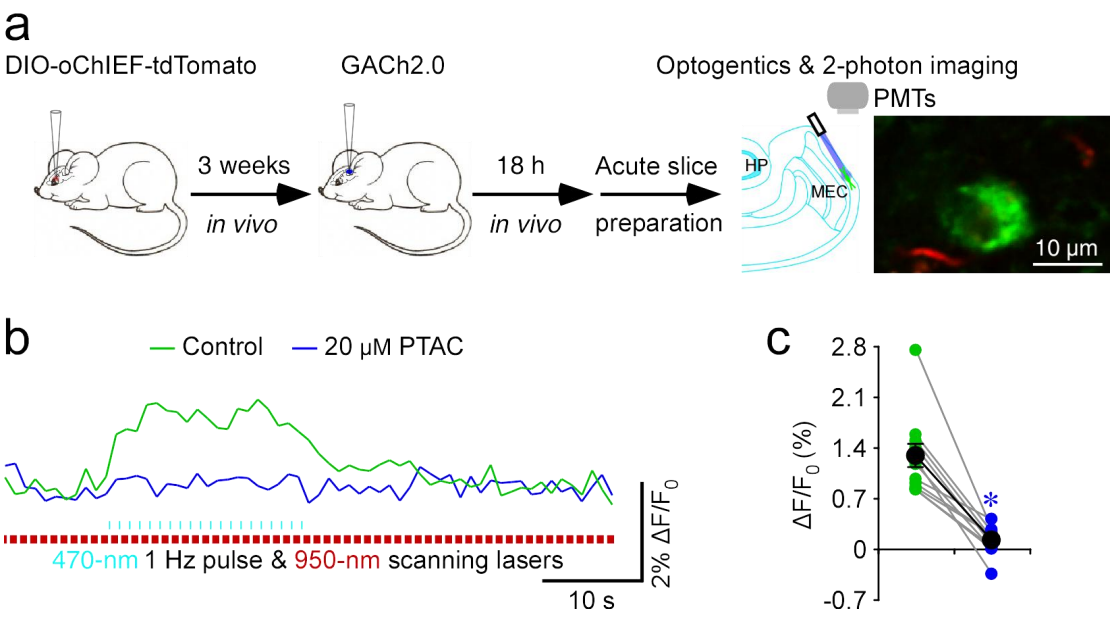

Supplementary figure 20: GACh2.0 provides an optical measurement of optogenetically evoked ACh release.

(**a**) Schematic drawing outlines the experimental design. Inserted images show a GACh2.0 expressing L2 stellate neuron and oChIEF-tdTomato expressing cholinergic fibers in MEC.

(**b**) Average $\Delta F/F_0$ responses of a GACh2.0 expressing neuron to optogenetic activation of cholinergic fibers originated from BF in the normal bath solution and bath solution containing 20 µM PTAC (*n* = 20 trials from the same neuron).

(**c**) Values for $\Delta F/F_0$ responses in the normal bath solution and bath solution containing 20 µM PTAC (Ctrl: 1.27 ± 0.15%; PTAC: 0.11 ± 0.05%, *Z* = -3.059; *p* = 0.002; *n* = 12 neurons from 11 animals).

Data are shown with mean ± s.e.m, with large black dots indicate mean responses, error bars indicate s.e.m.

Experiments in (**b**) were repeated independently for more than 10 animals with similar results.

*, $p < 0.05$ (Wilcoxon tests, two-sides).

Supplementary figure 21

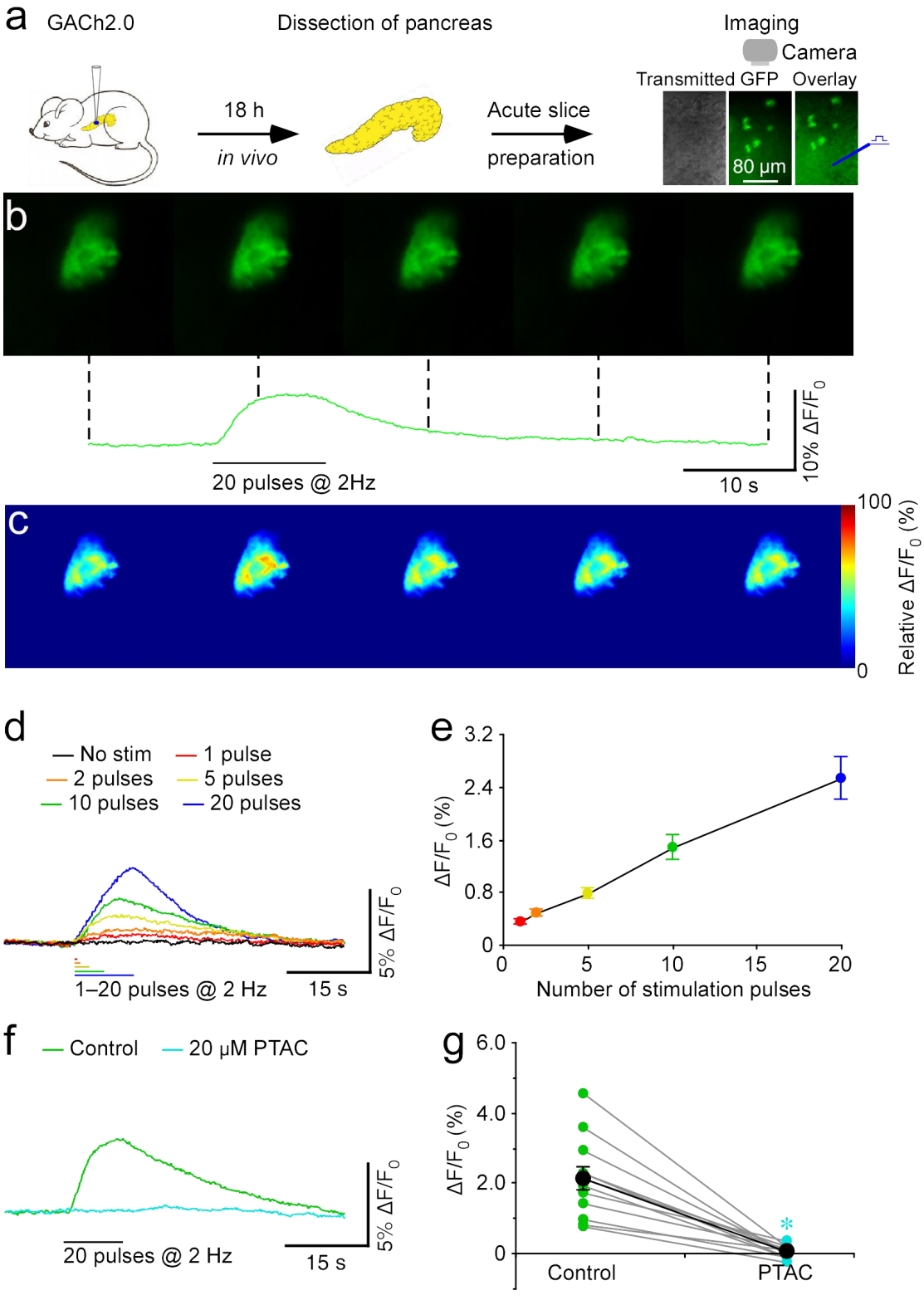

Supplementary figure 21: GACh2.0 permits visualization of cholinergic transmission in the pancreas.

(**a**) Schematic drawing outlines the design of stimulation-imaging experiments using an *in vivo* viral expression and *in vitro* mouse pancreas tissue slice preparation. Inserts show transmitted light (left), fluorescence microscopic (middle) and overlay (right) images of GACh2.0 expressing pancreatic cells.

(**b**) Snapshots of fluorescence responses of a GACh2.0 expressing pancreatic cell to local electrical stimulation.

(**c**) Relative fluorescence responses of the GACh2.0 expressing pancreatic cell to local electrical stimulation shown in a heat map format.

(**d**) Fluorescence responses of a GACh2.0 expressing pancreatic cell to electrical stimulations consisting of a train of up to 20 pulses at 2 Hz.

(**e**) Values for the maximal responses of GACh2.0 expressing pancreatic cells to electrical stimulations consisting of a train of up to 20 pulses at 2 Hz (2 pulses: 0.49 ± 0.05%, Z = 3.148, p = 0.001; 5 pulses: 0.78 ± 0.08%, Z = 3.527, p = 0.001; 10 pulses: 1.48 ± 0.19%, Z = 3.621, p = 0.001; 20 pulses: 2.53 ± 0.22%, Z = 3.621, p = 0.001; n = 17 neurons from 11 animals) compared to single pulses (1 pulse: 0.35 ± 0.04%).

(**f**) Electrically evoked fluorescence responses of GACh2.0 expressing pancreas cell bathed in the normal ACSF and ACSF containing 20 µM PTAC.

(**g**) Values for the maximal evoked responses of GACh2.0 expressing pancreas cells in presence of PTAC compared to control responses in normal ACSF (Ctrl: 2.11 ± 0.33%; Exp: 0.05 ± 0.05%, Z = -3.059, p = 0.001; n = 12 neurons from 5 animals).

Data are shown with mean ± s.e.m, with large black dots indicate mean responses, error bars indicate s.e.m.

Experiments in (**b**),(**c**),(**d**),(**f**) were repeated independently for more than 5 animals with similar results.

*, $p < 0.05$ (Wilcoxon tests, two-sides).

Supplementary figure 22

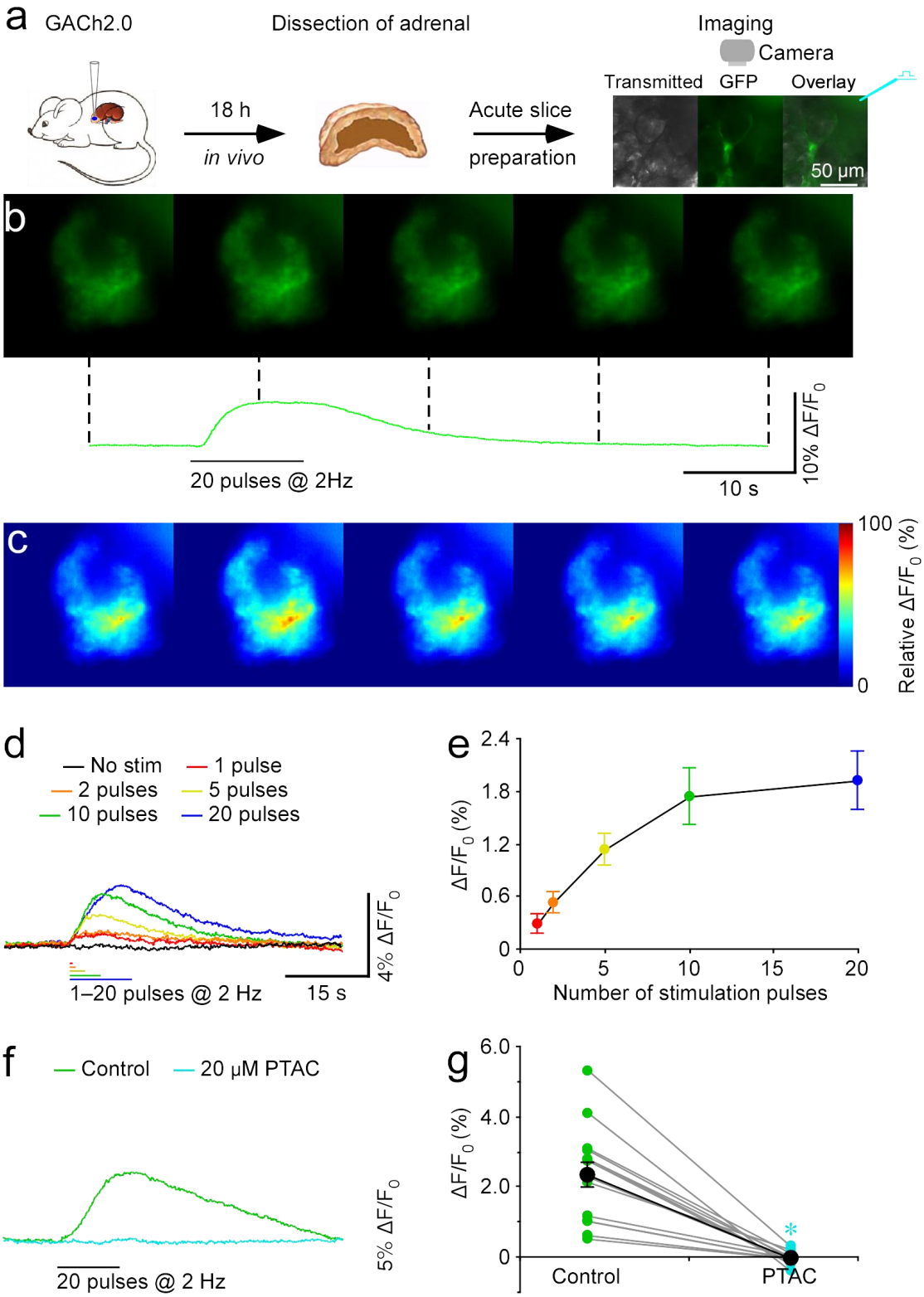

Supplementary figure 22: GACh2.0 visualizes cholinergic transmission in the adrenal gland.

(**a**) Schematic drawing outlines the design of stimulation-imaging experiments in the mouse adrenal. Inserts show transmitted light (left), fluorescence microscopic (middle) and overlay (right) images of a GACh2.0 expressing adrenal cell.

(**b**) Snapshot of fluorescence responses of a GACh2.0 expressing adrenal cell to local electrical stimulation.

(**c**) Relative fluorescence responses of the GACh2.0 expressing adrenal cell to local electrical stimulation shown in a heat map format.

(**d**) Fluorescence responses of GACh2.0 expressing adrenal cell to electrical stimulations consisting of a train of up to 20 pulses at 2 Hz.

(**e**) Values for the maximal responses of GACh2.0 expressing adrenal cells to electrical stimulations consisting of a train of up to 20 pulses at 2 Hz (2 pulses: 0.70 ± 0.14%, $Z = 2.981$, $p = 0.003$; 5 pulses: 1.27 ± 0.19%, $Z = 3.509$, $p = 0.003$; 10 pulses: 1.78 ± 0.25%, $Z = 3.509$, $p = 0.003$; 20 pulses: 1.94 ± 0.23%, $Z = 3.509$, $p = 0.003$; n = 12 neurons from 6 animals) compared to single pulses (1 pulse: 0.42 ± 0.11%).

(**f**) Electrically evoked fluorescence responses of GACh2.0 expressing adrenal cell in normal ACSF and ACSF containing 20 µM PTAC.

(**g**) Values for the maximal evoked responses of GACh2.0 expressing adrenal cells in presence of PTAC compared to control responses in normal ACSF (Ctrl: 2.32 ± 0.33%; PTAC: -0.02 ± 0.05%, $Z = -3.296$, $p = 0.001$; n = 14 neurons from 4 animals).

Data are shown with mean ± s.e.m, with large black dots indicate mean responses, error bars indicate s.e.m.

Experiments in (**b**),(**c**),(**d**),(**f**) were repeated independently for more than 4 animals with similar results.

*, $p < 0.05$ (Wilcoxon tests, two-sides).

Supplementary figure 23

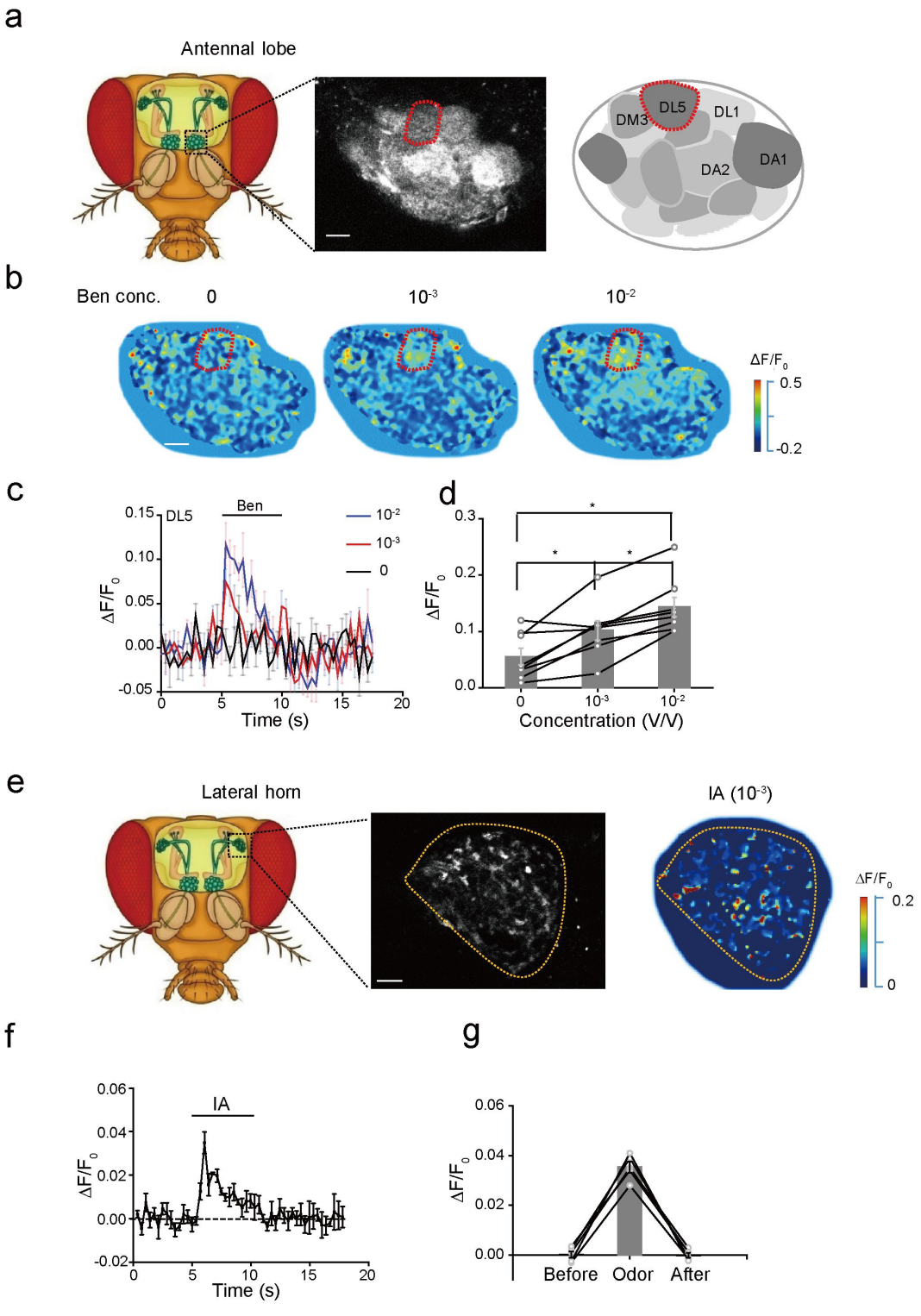

Supplementary figure 23: Odor-evoked GACh signals in *Drosophila* olfactory circuits, related to Fig. 5.

(**a**) Schematic illustration of the *Drosophila* olfactory system, where individual glomeruli in the antennal lobe were highlighted.

(**b**) Pseudocolor snapshots of the benzaldehyde-evoked GACh1.0 signals in the glomerular structure of antenna lobe (via GH146-Gal4>GACh1.0). Note the predominant action in DL5 glomerulus (red circle).

(**c**) Time courses of the benzaldehyde-evoked responses of DL5 glomerulus in (**b**). The traces were averaged from 3 trials in the same fly.

(**d**) Group data of the benzaldehyde-evoked $\Delta F/F_0$ in experiments of (**b**) (n = 8 flies, 10^{-3} Ben: 10.19 ± 1.69%, Z = 2.17, p = 0.029; 10^{-2} Ben: 14.32 ± 1.73%, Z = 2.45, p = 0.014) compared to control mineral oil (5.53 ± 1.47%). Z = 2.45, p = 0.014 between 10^{-2} Ben and 10^{-3} Ben.

(**e-g**) Similar experiments (as described in **a-d**) with IA-evoked responses measured in the lateral horn. The fluorescence signals of GACh1.0 to IA delivery were plotted in (**f**) and the group data of GACh1.0 signals before (first 5 seconds), during (IA, peak odor response, less than 1 second) and after (last 5 second) IA delivery were quantified in (**g**). N = 5 flies. $\Delta F/F_0$ of “before” (0.03 ± 0.13%, Z = -1.89, p = 0.06), “after” (0.010 ± 0.097%, Z = 1.89, p = 0.06) compared with “IA” (3.54 ± 0.23%). The fluorescence traces in (**f**) were averaged from 3 repeated trials in one fly.

Data are shown with mean ± s.e.m, with error bars indicate s.e.m. All scale bars, 10 μm.

Experiments in (**b**), (**e**) were repeated independently for more than 5 flies with similar results.

Wilcoxon test performed, two-sides.

Supplementary figure 24

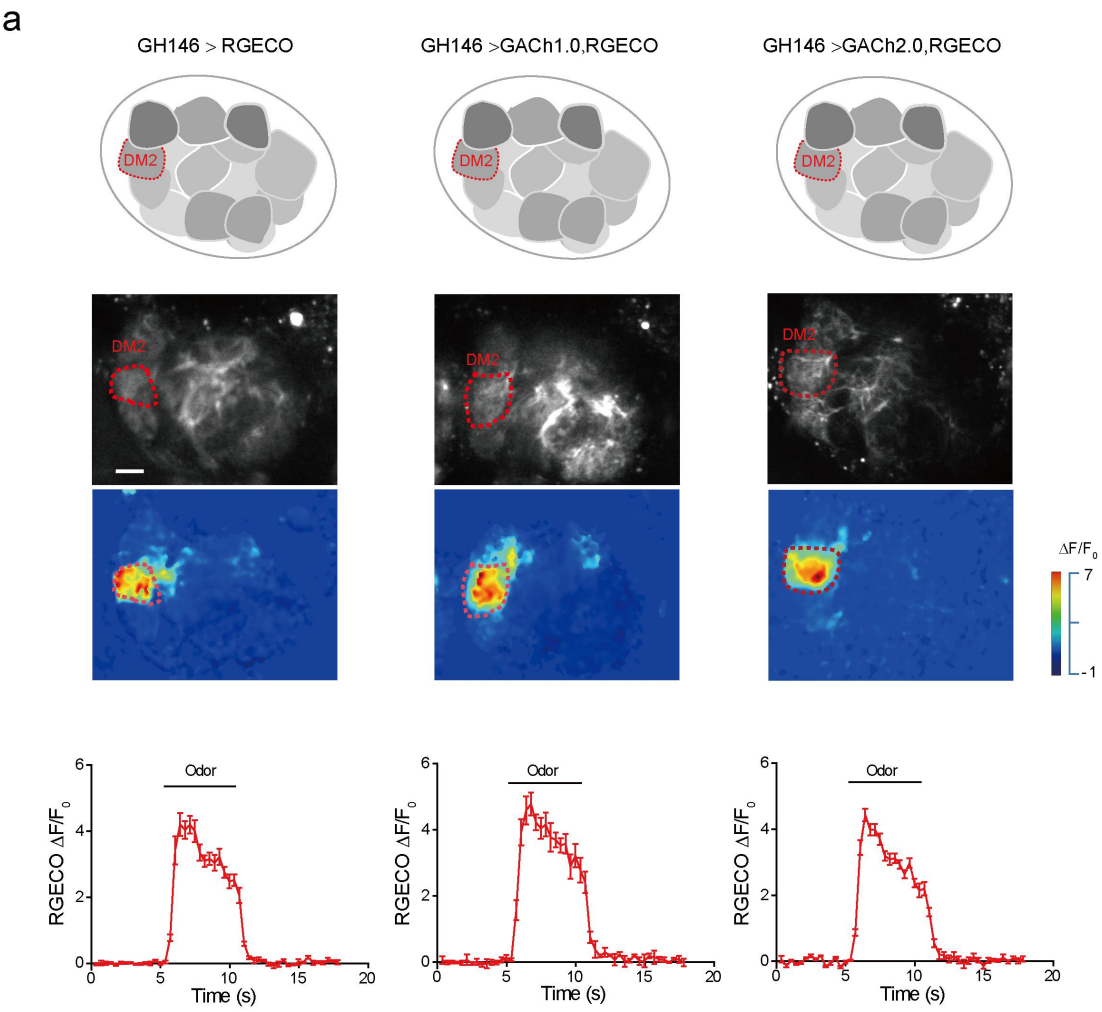

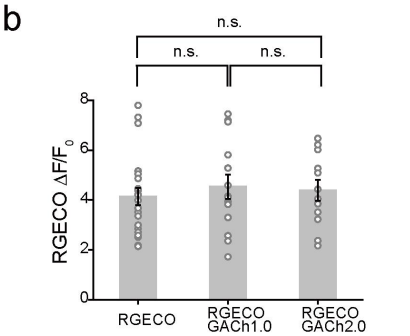

Supplementary figure 24: GACh sensors have no effect on the odor-evoked Ca^{2+} signaling in *Drosophila*.

(**a**) Upper, images exemplify the isoamyl acetate (IA)-evoked peak Ca^{2+} signals in control GH146 > RGECO transgenic, GH146 > GACh1.0,RGECO, and GH146 > GACh2.0,RGECO co-transgenic flies. Lower plots show the time course of Ca^{2+} signals in control GH146 > RGECO, GH146 > GACh1.0,RGECO, and GH146 > GACh2.0,RGECO flies (*n* = 3 repeated trials from the same fly).

(**b**) $\Delta F/F_0$ of the odor-evoked Ca^{2+} signals in control GH146 > RGECO and GH146 > GACh1.0,RGECO transgenic flies (GH146 > RGECO: 4.14 ± 0.34, *n* = 14 flies; GH146 > GACh1.0,RGECO: 4.53 ± 0.49, *n* = 22 flies, *U* = 139, *p* = 0.64 compared with GH146 > RGECO alone, GH146 > GACh2.0,RGECO: 4.38 ± 0.41, *n* = 12 flies, *U* = 115, *p* = 0.55 compared with GH146 > RGECO alone, *U* = 88, *p* = 0.86 compared with GH146 > GACh1.0,RGECO).

Data are shown with mean ± s.e.m, with error bars indicate s.e.m. All scale bars, 10 μm.

Experiments in (**b**), (**e**) were repeated independently for more than 5 flies with similar results.

n.s., not significant (Mann-Whitney Rank Sum non-parametric tests, two-sides).